Molecular Catalysis 510 (2021) 111660

Contents lists available at ScienceDirect

Molecular Catalysis

journal homepage: www.journals.elsevier.com/molecular-catalysis

C_2H_2 selective hydrogenation over the Cu_xM_y or Pd_xN_y intermetallic compounds: The influences of partner metal type and ratio on the catalytic performance

Wenjuan Zheng [a,b], Lixuan Ma [a,b], Baojun Wang [a,b], Jungang Wang [c], Riguang Zhang [a,b,*]

[a] State Key Laboratory of Clean and Efficient Coal Utilization, Taiyuan University of Technology, Taiyuan 030024, Shanxi, PR China
[b] Key Laboratory of Coal Science and Technology (Taiyuan University of Technology), Ministry of Education, PR China
[c] State Key Laboratory of Coal Conversion, Institute of Coal Chemistry, Chinese Academy of Sciences, Taiyuan 030001, Shanxi, PR China

ARTICLE INFO

Keywords:
Acetylene
Selective hydrogenation
Intermetallic compound
Partner metal
Catalytic performance

ABSTRACT

The Cu_xM_y and Pd_xN_y intermetallic compounds (IMCs) have exhibited better catalytic performance in hydrogenation reactions; however, for C_2H_2 selective hydrogenation, the most suitable partner metal type and ratio among Cu_xM_y and Pd_xN_y still remain unclear. This study investigated C_2H_2 selective hydrogenation on the Cu_xM_y(M = Zn, Pt, Ni, Pd, Au and Ag) and Pd_xN_y(N = Zn, Ga, In, Sn, Cu, Ag and Au) with different Cu/M and Pd/N ratios using density functional theory calculations, the results reveal that Cu_3Pd_1 IMCs with the surface isolated single-atom Pd anchored into the IMCs bulk as active center may serve as a promising catalyst for C_2H_2 selective hydrogenation due to industrially practical activity and selectivity for C_2H_4 formation, thermal stability, sufficient hydrogen source and green oil suppression, which is better than the previously reported single-atom Pd catalysts. This work would provide a guideline to design and screen out promising intermetallic compounds to catalyze selective hydrogenation of alkynes.

1. Introduction

In the process of C_2H_4 production by pyrolyzing petroleum hydrocarbons, trace C_2H_2 can be generated, which not only reduces the property of ethylene polymer, but also leads to the catalyst deactivation of C_2H_4 polymerization due to green oil formation, so trace C_2H_2 must be removed from the rich-feedstock C_2H_4 [1,2]. Commonly, C_2H_2 selective hydrogenation to C_2H_4 is an effective method [3,4]. Nowadays, Pd-based catalysts have been industrially used to catalyze the hydrogenation of C_2H_2 to C_2H_4 [5,6], however, the formation of the hydrides and carbide species for Pd-based catalysts are easy to deactivate the catalyst [7,8]. In recent years, Cu-based catalysts have attracted extensive interests due to high C_2H_4 selectivity [9,10]; however, they have low catalytic activity and favored the C—C polymerization to form green oil leading to catalyst deactivation [9,11]. Thus, developing the catalysts with high activity, high selectivity and high stability have attracted increasing interest [12–18]. Among them, the single-atom catalysts show excellent catalytic performance in C_2H_2 selective hydrogenation due to high activity and atomic utilization [15–18], however, the decreased stability of the single-atom catalysts and the easy occurrence of agglomeration also deactivate the catalyst [19].

Within the last ten decades, the intermetallic compounds (IMCs) have attracted extensive attention in catalytic hydrogenation due to their ordered atomic arrangement, unique electronic and structural characteristics, and excellent stability [20,21]. This type of catalyst can effectively separate active centers, and present unique catalytic performance [22–28]. For example, Wang *et al.* [24] experimentally showed Cu_xZn(x = 1,3) IMCs have better activity, selectivity, and higher stability for butadiene selective hydrogenation compared to Cu, which was ascribed to carbon deposit reduction. 4-aminophenylacetylene selectivity in 4-nitrophenylacetylene selective hydrogenation on PtZn IMCs is superior to that on the single-atom Pt and Pt nanoparticles, which is attributed to the easier adsorption of nitro groups by Zn atoms [25]. The experimentally prepared Ni_xM_y(M = Ga, Sn) IMCs with uniform size by Liu *et al.* [26] showed better C_2H_4 selectivity and the stability compared to Pd-based catalysts. Liu *et al.* [22] experimentally found an enhanced catalytic performance of CuNi IMCs for C_2H_2 selective hydrogenation due to the presence of isolated metal active center and the alloying effect of Ni and Cu. Zhou *et al.* [20] experimentally showed that Pd-Zn-Pd ensembles of PdZn IMCs promote H_2 dissociation and C_2H_4 desorption, which enhance C_2H_4 selectivity. Feng *et al.* [6] experimentally and

* Corresponding author.
E-mail addresses: zhangriguang@tyut.edu.cn, zhangriguang1981@163.com (R. Zhang).

https://doi.org/10.1016/j.mcat.2021.111660
Received 28 February 2021; Received in revised form 13 May 2021; Accepted 17 May 2021
Available online 7 June 2021

theoretically showed that PdIn(110) surface with the Pd single-atom as active centers has the elevated C_2H_4 selectivity.

As mentioned above, the intermetallic compounds have presented excellent catalytic performance toward selective hydrogenation reactions; moreover, some studies found the excellent catalytic performance of Cu or Pd intermetallic compounds toward C_2H_2 selective hydrogenation. However, to date, few studies have been carried out to examine the influences of the partner metal type and its ratio in the Cu or Pd intermetallic compounds on the catalytic performance of C_2H_2 hydrogenation, which still remain elusive; the surface structure characteristics of intermetallic compounds with excellent catalytic performance are also unclear. Further, the most suitable Cu or Pd intermetallic compounds remain unknown.

In order to solve above issues, this study is designed to perform a systematical study about C_2H_2 selective hydrogenation on a series of Cu and Pd intermetallic compounds with different partner metal types and ratios, which include the Cu_xM_y(M = Zn, Pt, Ni, Pd, Au and Ag) and Pd_xN_y(N = Zn, Ga, In, Sn, Cu, Ag and Au) IMCs corresponding to different Cu/M and Pd/N ratios of 1/1, 3/1 and 1/3. The results are expected to obtain the most suitable partner metal type and ratio among Cu_xM_y and Pd_xN_y IMCs catalysts with superior performance in C_2H_2 selective hydrogenation, and provide a guideline to design and screen out promising intermetallic compound catalysts for selective hydrogenation of alkynes.

2. Computational details

2.1. Computational method

The present DFT calculations were implemented by the Dmol^3 code [29,30] in Materials Studio 8.0 for Cu_xM_y(M = Zn, Pt, Pd, Au and Ag) and Pd_xN_y(N = Zn, Ga, In, Sn, Cu, Ag and Au) IMCs catalysts. The GGA and PBE [31,32] were applied to treat the exchange-correlation potential. The effective core potential (ECP) basis set was performed for IMCs, and the all-electron basis was applied to other species. The valence wave functions were expanded by the double-numeric polarized (DNP) basis set [33,34]. The *k*-points of (3 × 3 × 1) was used to handle surface models. A smearing width of 0.005 Ha was used. The transition states of C_2H_2 selective hydrogenation was obtained by the complete LST/QST technique [35,36]. TS confirmation and frequency analysis were implemented to confirm the structure of transition state.

2.2. Surface model

For the Cu IMCs, the Cu_xM_y(M = Pd, Pt, Au) with Cu/M ratio of 3/1, 1/3 and 1/1 [37–39] are considered, while for the Cu_xM_y(M = Zn, Ni), only the widely reported Cu/M ratios of 1/1 and 3/1 [24,40–44] are examined; the widely reported Cu_xAg_y corresponds to Cu/Ag ratio of 3/1 [41]. For the Pd IMCs, Pd_xN_y(N=Cu, Au and Ag) with Pd/N ratio of 3/1, 1/3 and 1/1 are considered [37], while Pd_xN_y(N = Zn, Ga) only considers the widely reported Pd/N ratio of 1/1 [27,45], Pd_xIn_y corresponds to Pd/In ratio of 1/1 and 3/1 [6,46], Pd_xSn_y corresponds to the ratio of 3/1 [47]. Further, in order to evaluate the catalytic performance of Cu IMCs and Pd IMCs catalysts in this study, Pd catalyst is selected as a reference. The optimized lattice parameters of Pd, Cu IMCs and Pd IMCs are summarized in Table S1, the calculated lattice parameters are close to the experimental values [27,37,39–41,43,46,47].

For the surface model, based on the low surface energy and dominantly exposed surface [6,27,43], the *p*(3 × 3) (110) surface is selected for the Cu_1Zn_1, the *p*(3 × 3) (111) surface is selected for the Cu_3Zn_1, Cu_1Pt_1, Cu_3Pt_1, Cu_1Pt_3, Cu_1Ni_1, Cu_3Ni_1, Cu_1Pd_1, Cu_3Pd_1, Cu_1Pd_3, Cu_1Au_1, Cu_3Au_1, Cu_1Au_3, Cu_3Ag_1, Pd_1Zn_1, Pd_3In_1, Pd_3Sn_1, Pd_1Ag_1, Pd_3Ag_1, Pd_1Ag_3, Pd_1Au_1, Pd_3Au_1, Pd_1Au_3 and Pd; the *p*(3 × 2) (110) and *p*(4 × 2) (110) surfaces are selected for Pd_1Ga_1 and Pd_1In_1 IMCs, respectively. All catalysts contain four atomic layers except for PdGa(110) with seven atomic layers. The bottom two layers for all surfaces are fixed except for PdGa(110) surface with the bottom four layers fixed. A vacuum region of 15 Å is set to separate the periodic slabs. Fig. 1 shows the optimized model surfaces of Cu IMCs, Pd IMCs and Pd.

3. Results and discussion

3.1. The possible routes of C_2H_2 selective hydrogenation

As shown in Fig. 2, C_2H_2 selective hydrogenation includes the processes of the hydrogenation and polymerization. For the hydrogenation process, three possible routes exist, the first is ***C_2H_4 desorption route*** that C_2H_2(ad) is firstly hydrogenated via C_2H_3(ad) intermediate to generate C_2H_4(ad), followed by its desorption from the catalyst surface; the second is ***C_2H_4 hydrogenation route*** that C_2H_2(ad) is excessively hydrogenated to C_2H_5(ad) through C_2H_4 intermediate; the third is ***$CHCH_3$ hydrogenation route*** that C_2H_2(ad) is excessively hydrogenated to C_2H_5(ad) through $CHCH_3$ intermediate. The route of C_2H_4 desorption is the desired route to realize the removal of trace C_2H_2 in rich-C_2H_4 stream.

Based on above analysis, the first is to determine the preference between C_2H_4 hydrogenation and its desorption by comparing the activation free energy between C_2H_4 hydrogenation and its desorption. Then, when C_2H_4 desorption route is favored, starting from the common intermediate C_2H_3 in three routes, the preference between C_2H_4 formation and $CHCH_3$ formation is examined. Finally, the catalysts that can produce gaseous C_2H_4 are screened out.

For the polymerization process, green oil is formed to block active centers and deactivate the catalysts. Most studies have shown that the precursor for the production of green oil is 1,3-butadiene [1,2,48], thus, three possible routes of 1,3-butadiene formation are investigated, the first is the coupling of adsorbed C_2H_2 to C_4H_4, followed by its hydrogenation to C_4H_6; the second is the coupling of adsorbed C_2H_2 and C_2H_3 to C_4H_5, followed by its hydrogenation to C_4H_6; the third is the coupling of adsorbed C_2H_3 to C_4H_6.

3.2. C_2H_2 selective hydrogenation on the Cu IMCs catalysts

3.2.1. The adsorption of C_2H_2 and C_2H_4

Since the amount of C_2H_2 in the C_2H_4-rich stream is very small, C_2H_2 must be strongly adsorbed on the catalyst than C_2H_4 to ensure the subsequent hydrogenation of C_2H_2. The most stable configurations of C_2H_2 and C_2H_4 on the Cu_xM_y(M = Zn, Pt, Ni, Pd, Au and Ag) IMCs are shown in Fig. S2.

As shown in Fig. 3a, on the Cu_1Au_1 and Cu_1Au_3 IMCs, the adsorption strength of C_2H_2 (37.2 and 16.1 kJ·mol^{-1}) and C_2H_4 (1.1 and 1.9 kJ·mol^{-1}) is very weak physisorption, namely, both Cu_1Au_1 and Cu_1Au_3 cannot validly adsorb trace C_2H_2 in rich-C_2H_4 stream, and therefore C_2H_2 selective hydrogenation cannot be performed. However, C_2H_2 has much higher adsorption energy at 425 K than C_2H_4 on other twelve types of Cu IMCs catalysts, including Cu_1Zn_1, Cu_3Zn_1, Cu_1Pt_1, Cu_3Pt_1, Cu_1Pt_3, Cu_1Ni_1, Cu_3Ni_1, Cu_1Pd_1, Cu_3Pd_1, Cu_1Pd_3, Cu_3Au_1 and Cu_3Ag_1, indicating that these twelve types of Cu IMCs catalysts favor C_2H_2 selective hydrogenation. Further, the adsorption energies and the stable configurations at 425 K of H, C_2H_3, $CHCH_3$ and C_2H_5 species on twelve types of Cu IMCs are presented in Table S2 and Fig. S3.

3.2.2. The preference between C_2H_4 desorption and its hydrogenation

Based on above analysis, the preference between C_2H_4 hydrogenation and C_2H_4 desorption is further examined on above twelve types of Cu IMCs catalysts, as shown in Fig. 4. Among them, only on Cu_1Pt_3, C_2H_4 desorption is competitive with its hydrogenation (80.2 *vs.* 87.4 kJ·mol^{-1}, Fig. 4e); whereas C_2H_4 prefers to desorb rather than its hydrogenation to C_2H_5 on other eleven types of Cu IMCs catalysts, including Cu_1Zn_1, Cu_3Zn_1, Cu_1Pt_1, Cu_3Pt_1, Cu_1Ni_1, Cu_3Ni_1, Cu_1Pd_1, Cu_3Pd_1, Cu_1Pd_3, Cu_3Au_1 and Cu_3Ag_1. Further, previous studies by Xu *et al.* [37] also showed that C_2H_4 desorption prefers to occur rather than its hydrogenation over the three-layers *p*(4 × 4) (111) surfaces of Cu_1Pt_1 and Cu_3Pt_1 IMCs at 473 K;

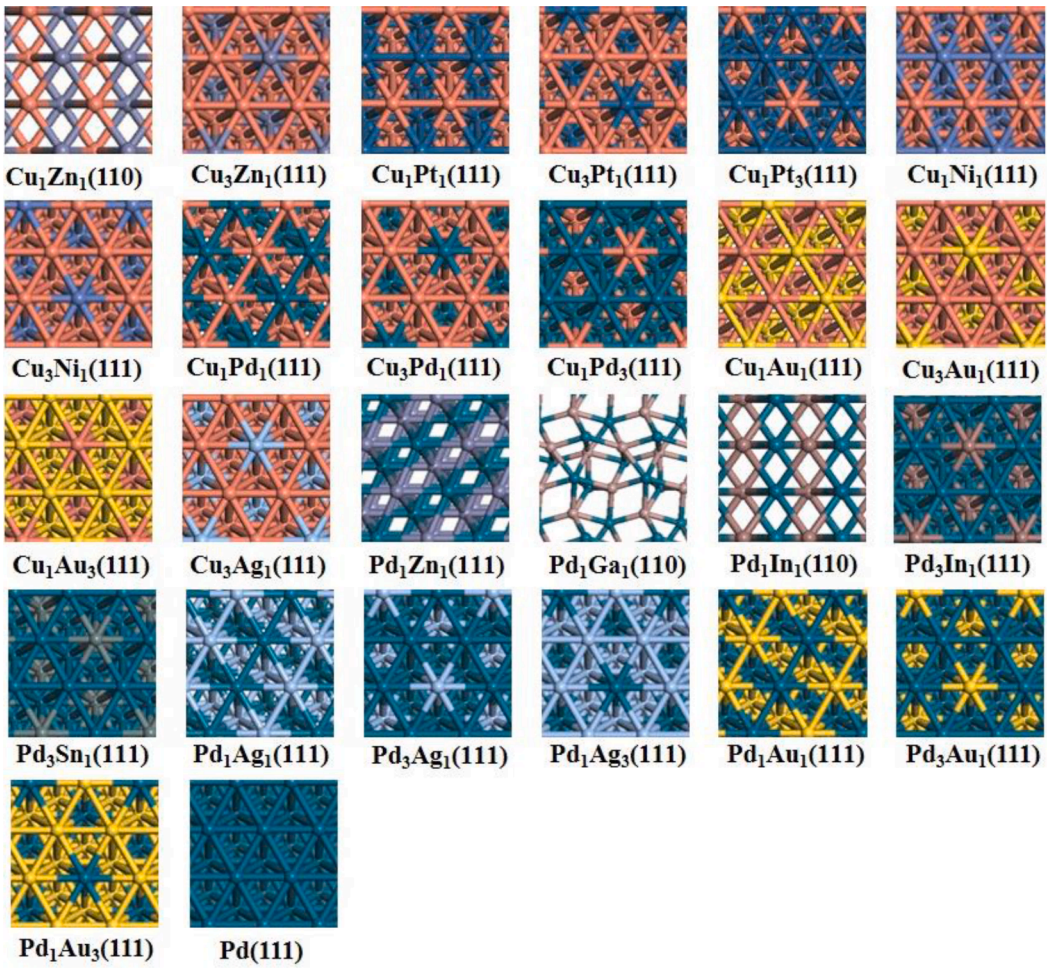

Fig. 1. The optimized surface structures of Cu_xM_y(M = Zn, Pt, Ni, Pd, Au, Ag), Pd_xN_y(N = Zn, Ga, In, Sn, Cu, Ag, Au) IMCs and Pd catalysts.

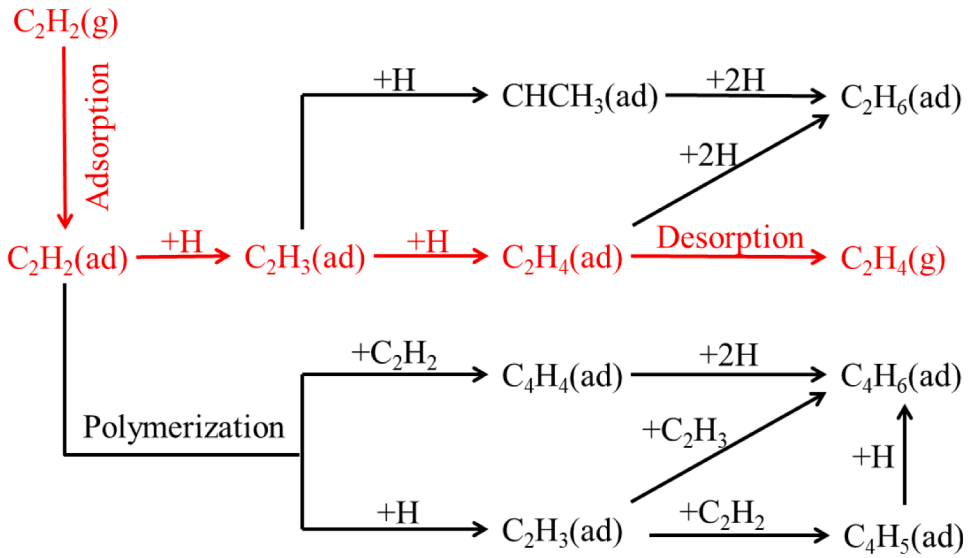

Fig. 2. The possible reaction pathways of C_2H_2 selective hydrogenation including the hydrogenation and polymerization processes. (ad) stands for the adsorbed state, and (g) stands for the gas phase state, respectively.

the same results are also obtained by Wang *et al.* [49] on the three-layer *p* (3 × 3) (111) surfaces of Cu_1Pd_1, Cu_3Pd_1 and Cu_1Pd_3 IMCs at 400 K. Liu *et al.* [22] experimently showed that the homogeneous CuNi alloy is in favor of gaseous C_2H_4 formation.

3.2.3. *The preference between C_2H_4 formation and $CHCH_3$ formation*

As mentioned above, except for Cu_1Pt_3 IMCs, other eleven types of Cu IMCs are conducive to C_2H_4 desorption rather than being hydrogenated. Thus, starting from the common intermediate C_2H_3 in three routes, we

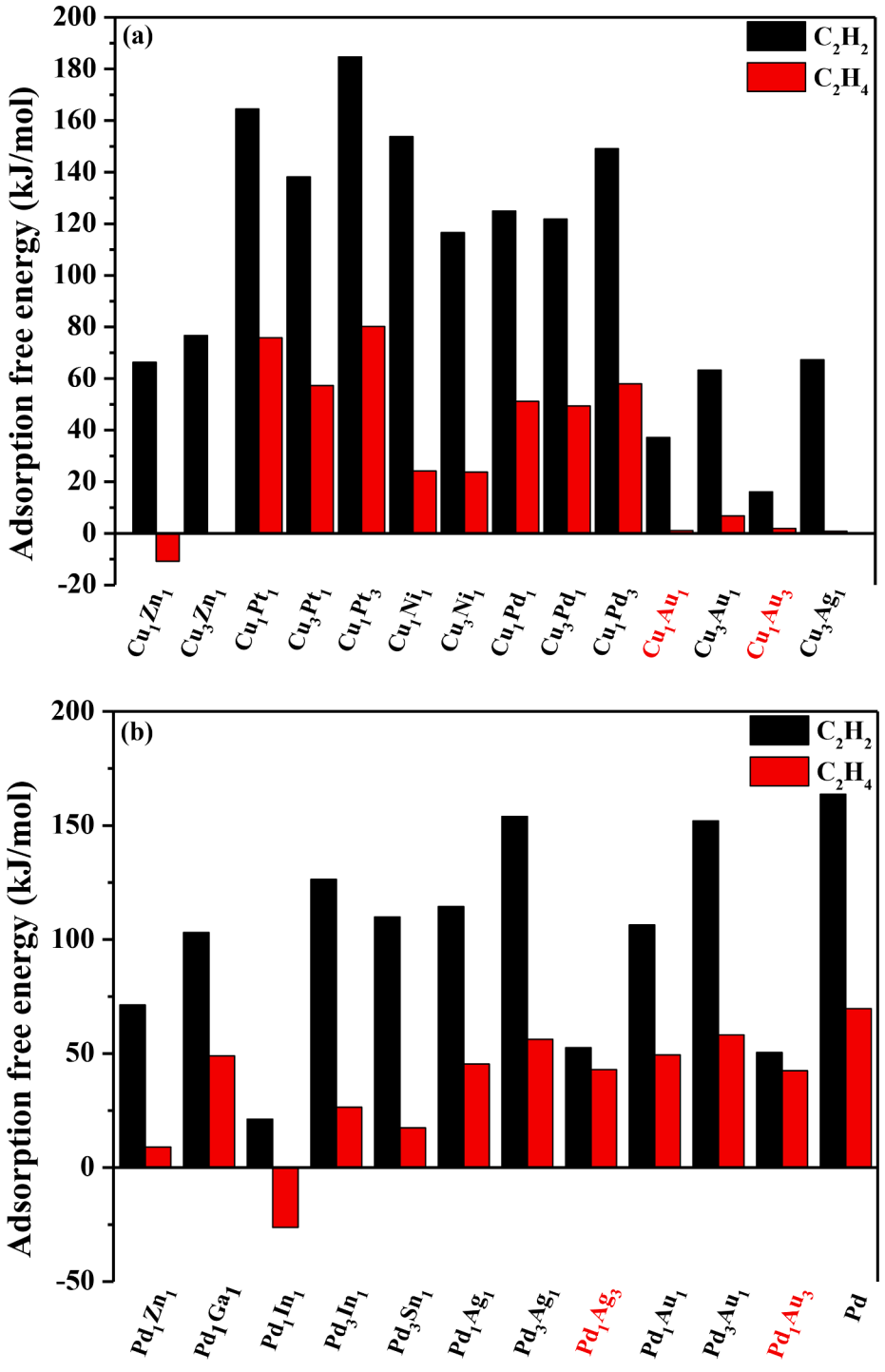

Fig. 3. The adsorption free energies of C_2H_2 and C_2H_4 species over the (a) Cu_xM_y(M = Zn, Pt, Ni, Pd, Au, Ag) and (b) Pd_xN_y(N = Zn, Ga, In, Sn, Ag, Au) IMCs and Pd catalysts at 425 K.

further determine whether C_2H_4 is more easily formed than $CHCH_3$ in C_2H_3 hydrogenation (see Figs. S4~S8).

For the Cu_xZn_y IMCs, C_2H_3 hydrogenation to C_2H_4 is kinetically more favorable than its hydrogenation to $CHCH_3$ on the Cu_1Zn_1 (40.8 *vs.* 180.6 kJ·mol^{-1}, Fig. S4a) and Cu_3Zn_1 (65.6 *vs.* 204.7 kJ·mol^{-1}, Fig. S4b). The same thing also occurs on the Cu_1Pt_1, Cu_3Pt_1, Cu_1Ni_1, Cu_3Ni_1, Cu_1Pd_1, Cu_3Pd_1, Cu_3Au_1 and Cu_3Ag_1, as presented in Figs. S5~S8. However, it is opposite on Cu_1Pd_3 (109.4 *vs.* 94.4 kJ·mol^{-1}, Fig. S7c), while $CHCH_3$ hydrogenation to C_2H_5 is more difficult compared to C_2H_4 formation and desorption (170.4 *vs.* 109.4 kJ·mol^{-1}, Fig. S7c), thus, $CHCH_3$ hydrogenation route is unfavorable on Cu_1Pd_3, which agree with the previous work by Wang *et al.* [49] on the three-layer $p(3 \times 3)$ (111) surfaces of Cu_1Pd_1, Cu_3Pd_1 and Cu_1Pd_3 IMCs at 400 K.

Above results show that eleven types of Cu IMCs, including Cu_1Zn_1, Cu_3Zn_1, Cu_1Pt_1, Cu_3Pt_1, Cu_1Ni_1, Cu_3Ni_1, Cu_1Pd_1, Cu_3Pd_1, Cu_3Au_1, Cu_3Ag_1 and Cu_1Pd_3, preferentially favor C_2H_2 hydrogenation to C_2H_4 and its subsequent desorption. Namely, C_2H_4 desorption route to produce gaseous C_2H_4 is dominant.

3.2.4. C_2H_4 formation activity and selectivity

Since eleven types of Cu_xM_y(M = Zn, Pt, Ni, Pd, Au and Ag) IMCs favor the production of gaseous C_2H_4, C_2H_4 formation activity and selectivity

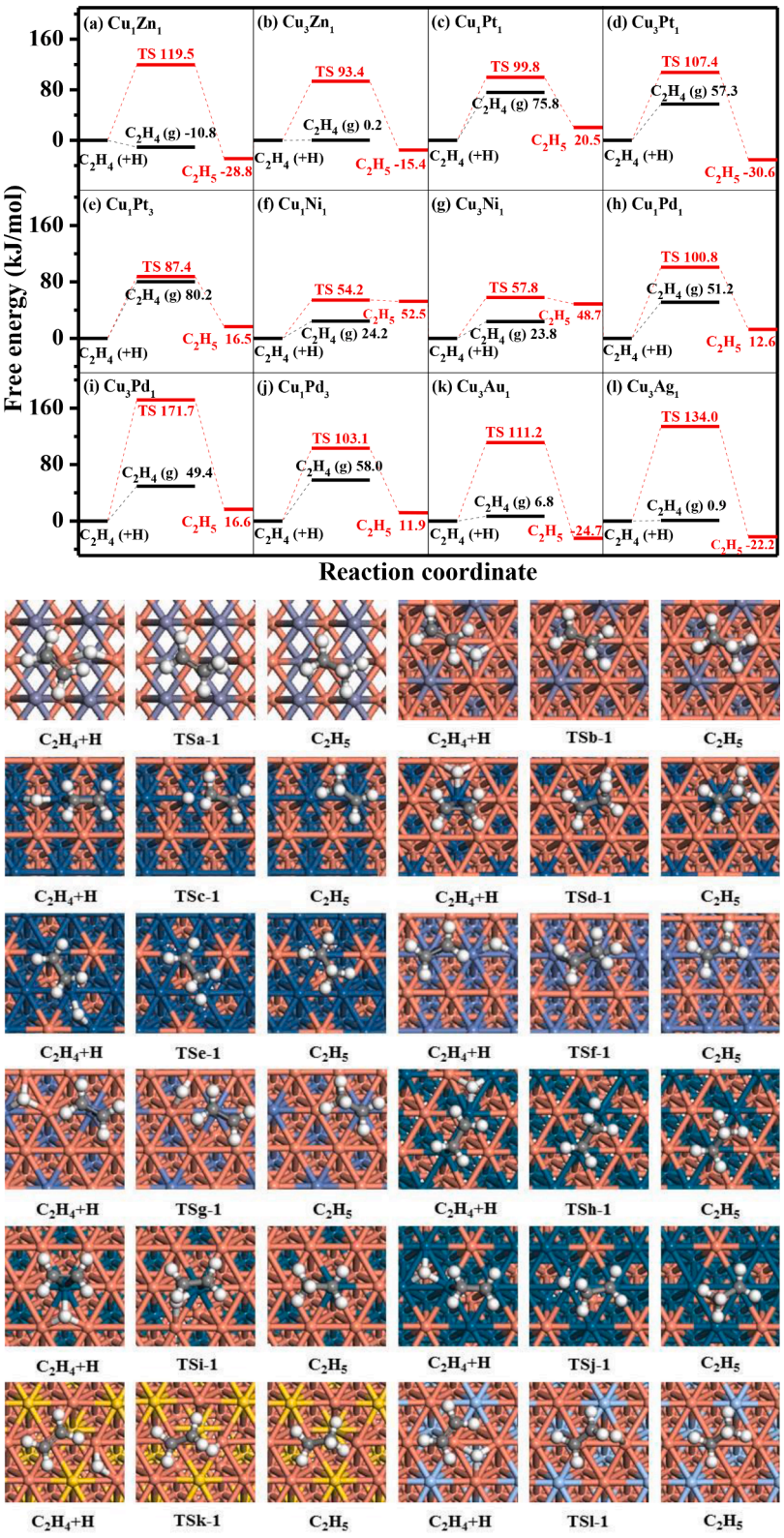

Fig. 4. The potential energy profile at 425 K of C_2H_4 hydrogenation and C_2H_4 desorption together with the initial state, transition state and final state on the (a) Cu_1Zn_1, (b) Cu_3Zn_1, (c) Cu_1Pt_1, (d) Cu_3Pt_1, (e) Cu_1Pt_3, (f) Cu_1Ni_1, (g) Cu_3Ni_1, (h) Cu_1Pd_1, (i) Cu_3Pd_1, (j) Cu_1Pd_3, (k) Cu_3Au_1 and (l) Cu_3Ag_1, respectively.

over these catalysts are calculated to evaluate the catalytic performance [37,50,51].

In this study, the descriptor, the energy difference between C_2H_4 hydrogenation and its desorption, is used to evaluate C_2H_4 selectivity, this descriptor as the simplest way can well quantitatively and qualitatively evaluate C_2H_4 selectivity in C_2H_2 selective hydrogenation, which has been widely used in the previous studies by Hu *et al.* [8,51–54], Mavrikakis *et al.* [37], Celik *et al.* [55], Hafner *et al.* [56], Kang *et al.* [18], Wang *et al.* [57,58] and Gong *et al.* [1], the obtained results can well present C_2H_4 selectivity over the reported catalysts and agrees with the experimental

results. Meanwhile, C_2H_4 formation rate is calculated to evaluate C_2H_4 formation activity [59,60], which is calculated according to a two-step model [8,61] under the typically experimental conditions (T = 425 K, P = 1 atm; the partial pressure of C_2H_2, H_2 and C_2H_4 correspond to 0.01, 0.1 and 0.89 atm, respectively) (the details are presented in the Supplementary Material).

As listed in Table 1, eleven types of Cu IMCs catalysts correspond to C_2H_4 selectivity of 130.3, 93.2, 24.0, 50.1, 30.0, 34.0, 49.6, **122.3**, 45.1, 104.4 and 133.1 kJ·mol^{-1}; correspondingly, C_2H_4 formation activity of 1.21×10^{-4}, 5.27×10^{-1}, 8.85×10^{1}, 8.08×10^{-4}, 8.87×10^{-2}, 1.33×10^{1}, 2.30×10^{-3}, $\mathbf{4.77 \times 10^{6}}$, 3.17×10^{-1}, 4.45×10^{-4} and 5.68×10^{0} s^{-1}·site^{-1} on the Cu_1Zn_1, Cu_3Zn_1, Cu_1Pt_1, Cu_3Pt_1, Cu_1Ni_1, Cu_3Ni_1, Cu_1Pd_1, Cu_3Pd_1, Cu_1Pd_3, Cu_3Au_1 and Cu_3Ag_1, respectively.

Above results show that Cu_3Pd_1 with the isolated single-atom Pd as active center exhibits outstanding C_2H_4 selectivity and activity (**122.3** kJ·mol^{-1} and $\mathbf{4.77 \times 10^{6}}$ s^{-1}·site^{-1}). Hence, Cu_3Pd_1 can better promote C_2H_4 formation.

3.2.5. The influences of partner metal ratio and metal type on C_2H_4 formation

Based on above results, among Cu_xM_y(M = Zn, Pt, Ni, Pd, Au and Ag) IMCs, the Cu_xPd_y, Cu_xAg_y, Cu_xAu_y and Cu_xNi_y IMCs corresponding to Cu/Pd, Cu/Ag, Cu/Au and Cu/Ni ratio of 3/1 have better C_2H_4 formation activity and selectivity than the other Cu/M(M = Pd, Ag, Au and Ni) ratios; however, the Cu_xZn_y with the Cu/Zn ratio of 3/1 and Cu_xPt_y with the Cu/Pt ratio of 1/1 have high activity of C_2H_4 formation, whereas the Cu_xZn_y with the Cu/Zn ratio of 1/1 and Cu_xPt_y with the Cu/Pt ratio of 3/1 have high C_2H_4 selectivity. Thus, the partner metal ratio of Cu_xM_y(M = Zn, Pt, Ni, Pd, Au and Ag) IMCs has a significant influence on C_2H_4 formation activity and selectivity. In addition, NiGa IMCs has better activity and selectivity than Ni and Ni_3Ga IMCs for C_2H_2 selective hydrogenation to C_2H_4 [23]. PdIn presented better selectivity than Pd_3In and Pd for HCOOH oxidation [62]. Ni_3Sn_2 displays the best furfuryl alcohol selectivity and its formation activity for furfural selective hydrogenation on the Ni_3Sn_1, Ni_3Sn_2 and Ni_3Sn_4 IMCs [63]. Further, as shown in Fig. 6, the partner metal type M (M = Zn, Pt, Ni, Pd, Au and Ag) in the Cu_xM_y IMCs catalysts affects C_2H_4 formation activity and selectivity, among them, Cu_3Pd_1 catalyst displays remarkably high C_2H_4 formation activity and selectivity compared to other Cu_xM_y IMCs catalysts, suggesting that Cu_3Pd_1 IMCs doped the partner metal Pd into Cu is the best choice for C_2H_2 selective hydrogenation among Cu_xM_y IMCs. In addition, CuNi(111) is more favorable for carbon elimination than FeNi (111) and Ni(111) [40]. Wang *et al.* [49] found that $PdCu_3$ displays the highest C_2H_4 formation activity and selectivity among PdCu, PdAg and PdAu IMCs.

Table 1
The calculated adsorption free energies (G_{ads}/kJ·mol^{-1}) of C_2H_2 and C_2H_4, the activation barriers (G_a/kJ·mol^{-1}) of C_2H_4 hydrogenation to C_2H_5, C_2H_4 selectivity (G_{sel}/kJ·mol^{-1}) and the reaction rate of C_2H_4 formation (r/s^{-1}·site^{-1}) in C_2H_2 selective hydrogenation over the Cu_xM_y and Pd_xN_y IMCs and Pd catalysts at 425 K except for the Cu_1Au_1, Cu_1Au_3, Pd_1Ag_3 and Pd_1Au_3 catalysts that cannot achieve effective adsorption of trace C_2H_2 in C_2H_4-rich streams, and Cu_1Pt_3 catalyst with C_2H_4 desorption competitive with its hydrogenation.

Catalysts	$G_{ads}(C_2H_2)$	$G_{ads}(C_2H_4)$	G_a	G_{sel}	r
Cu_1Zn_1(110)	66.3	-10.8	119.5	130.3	1.21×10^{-4}
Cu_3Zn_1(111)	76.7	0.2	93.4	93.2	5.27×10^{-1}
Cu_1Pt_1(111)	164.5	75.8	99.8	24.0	8.85×10^{1}
Cu_3Pt_1(111)	138.2	57.3	107.4	50.1	8.08×10^{-4}
Cu_1Pt_3(111)	184.6	80.2	—	—	—
Cu_1Ni_1(111)	153.8	24.2	54.2	30.0	8.87×10^{-2}
Cu_3Ni_1(111)	116.6	23.8	57.8	34.0	1.33×10^{1}
Cu_1Pd_1(111)	124.9	51.2	100.8	49.6	2.30×10^{-3}
Cu_3Pd_1(111)	121.8	49.4	171.7	122.3	4.77×10^{6}
Cu_1Pd_3(111)	149.1	58.0	103.1	45.1	3.17×10^{-1}
Cu_1Au_1(111)	37.2	1.1	—	—	—
Cu_3Au_1(111)	63.3	6.8	111.2	104.4	4.45×10^{-4}
Cu_1Au_3(111)	16.1	1.9	—	—	—
Cu_3Ag_1(111)	67.3	0.9	134.0	133.1	5.68×10^{0}
Pd_1Zn_1(111)	71.3	9.0	92.6	83.6	2.57×10^{0}
Pd_1Ga_1(110)	103.1	49.0	211.7	162.7	1.20×10^{-3}
Pd_1In_1(110)	21.2	-26.2	190.8	217.0	2.05×10^{0}
Pd_3In_1(111)	126.4	26.5	141.5	115.0	1.23×10^{-5}
Pd_3Sn_1(111)	109.9	17.4	143.0	125.6	9.38×10^{-2}
Pd_1Ag_1(111)	114.5	45.4	89.5	44.1	4.41×10^{0}
Pd_3Ag_1(111)	154.0	56.2	116.3	60.1	5.92×10^{-4}
Pd_1Ag_3(111)	52.6	43.0	—	—	—
Pd_1Au_1(111)	106.4	49.4	85.4	36.0	3.01×10^{4}
Pd_3Au_1(111)	152.0	58.2	87.7	29.5	5.12×10^{2}
Pd_1Au_3(111)	50.5	42.5	—	—	—
Pd(111)	163.7	69.7	88.6	18.9	3.55×10^{-1}

3.3. C_2H_2 selective hydrogenation on the Pd IMCs catalysts

3.3.1. The adsorption of C_2H_2 and C_2H_4

Similar to Cu IMCs, the adsorptions of C_2H_2 and C_2H_4 on the Pd_xN_y(N = Zn, Ga, In, Sn, Cu, Ag and Au) IMCs and Pd catalysts are examined (see details in Fig. S2). As shown in Fig. 3b, the adsorption free energy of C_2H_2 and C_2H_4 on the Pd_1Ag_3 (52.6 and 43.0 kJ·mol^{-1}) and Pd_1Au_3 (50.5 and 42.5 kJ·mol^{-1}) is very close, which is not in favor of the effective adsorption of the trace C_2H_2 in a large amount of C_2H_4. However, C_2H_2 has much larger adsorption energy than C_2H_4 on the Pd_1Zn_1, Pd_1Ga_1, Pd_1In_1, Pd_3In_1, Pd_3Sn_1, Pd_1Cu_1, Pd_3Cu_1, Pd_1Cu_3, Pd_1Ag_1, Pd_3Ag_1, Pd_1Au_1, Pd_3Au_1 and Pd at 425 K. Namely, C_2H_2 is more strongly adsorbed than C_2H_4 on above twelve types of Pd IMCs and Pd catalysts. Correspondingly, the adsorption energies and stable adsorption configurations at 425 K of H, C_2H_3, $CHCH_3$ and C_2H_5 species on twelve types of Pd IMCs and Pd catalysts are presented in Table S2 and Fig. S3.

3.3.2. The preference between C_2H_4 desorption and its hydrogenation

As mentioned above, the preference between C_2H_4 hydrogenation and its desorption is further examined on twelve types of Pd IMCs and Pd. As presented in Fig. 5, C_2H_4 desorption occurs more easily compared to its hydrogenation on the Pd_1Zn_1, Pd_1Ga_1, Pd_1In_1, Pd_3In_1, Pd_3Sn_1, Pd_1Ag_1, Pd_3Ag_1, Pd_1Au_1, Pd_3Au_1 and Pd. The same thing also occurs on the Pd_1Cu_1 (Fig. 4h), Pd_1Cu_3 (Fig. 4i) and Pd_3Cu_1 (Fig. 4j). Thus, the desorption of C_2H_4 is more favorable on these twelve types of Pd IMCs and Pd catalyst. Previous studies also showed that C_2H_4 desorption (48.0 kJ·mol^{-1}) is easier than its hydrogenation (84.0 kJ·mol^{-1}) on PdZn(100) IMCs at 0 K [20]; the same results also occur on the three-layer $p(3 \times 3)$ (111) surfaces of Pd_1Ag_1, Pd_3Ag_1, Pd_1Au_1 and Pd_3Au_1 IMCs at 400 K [49].

3.3.3. The preference between C_2H_4 formation and $CHCH_3$ formation

For the Pd_xN_y IMCs (see Figs. S9~S14), C_2H_3 is preferentially hydrogenated to generate C_2H_4 rather than $CHCH_3$ on the Pd_1Zn_1 (Fig. S9a), Pd_1Ga_1 (Fig. S9b), Pd_1In_1 (Fig. S10a), Pd_3In_1 (Fig. S10b), Pd_3Sn_1 (Fig. S11), Pd_1Ag_1 (Fig S12a) and Pd_1Au_1 (Fig. S13a); the same thing also occurs on the Pd_1Cu_1 (Fig. S7a) and Pd_1Cu_3 (Fig. S7b). On the other hand, it is opposite on the Pd_3Cu_1 (Fig. S7c), Pd_3Ag_1 (Fig S12b), Pd_3Au_1 (Fig. S13b) and Pd (Fig. S14), however, $CHCH_3$ hydrogenation to C_2H_5 is more difficult than C_2H_4 formation and desorption on the Pd_3Cu_1 (170.4 *vs.* 109.4 kJ·mol^{-1}, Fig. S7c), Pd_3Ag_1 (173.7 *vs.* 131.6 kJ·mol^{-1}, Fig. S12b), Pd_3Au_1 (89.7 *vs.* 83.3 kJ·mol^{-1}, Fig. S13b) and Pd (126.9 *vs.* 109.0 kJ·mol^{-1}, Fig. S14), thus, $CHCH_3$ hydrogenation route is not easy to occur.

Above results show that C_2H_3 hydrogenation to C_2H_4 and C_2H_4 desorption are favored on above twelve types of Pd IMCs and Pd catalysts, namely, C_2H_4 desorption route to form gaseous C_2H_4 is dominant among three hydrogenation routes.

3.3.4. C_2H_4 formation activity and selectivity

As illustrated in Table 1, on twelve types of Pd_xN_y(N = Zn, Ga, In, Sn, Cu, Ag and Au) IMCs and Pd catalysts, C_2H_4 selectivity is 83.6, 162.7, 217.0, 115.0, 125.6, 49.6, 45.1, **122.3**, 44.1, 60.1, 36.0, 29.5 and 18.9 kJ·mol^{-1} on the Pd_1Zn_1, Pd_1Ga_1, Pd_1In_1, Pd_3In_1, Pd_3Sn_1, Pd_1Cu_1, Pd_3Cu_1, Pd_1Cu_3, Pd_1Ag_1, Pd_3Ag_1, Pd_1Au_1, Pd_3Au_1 and Pd catalysts.

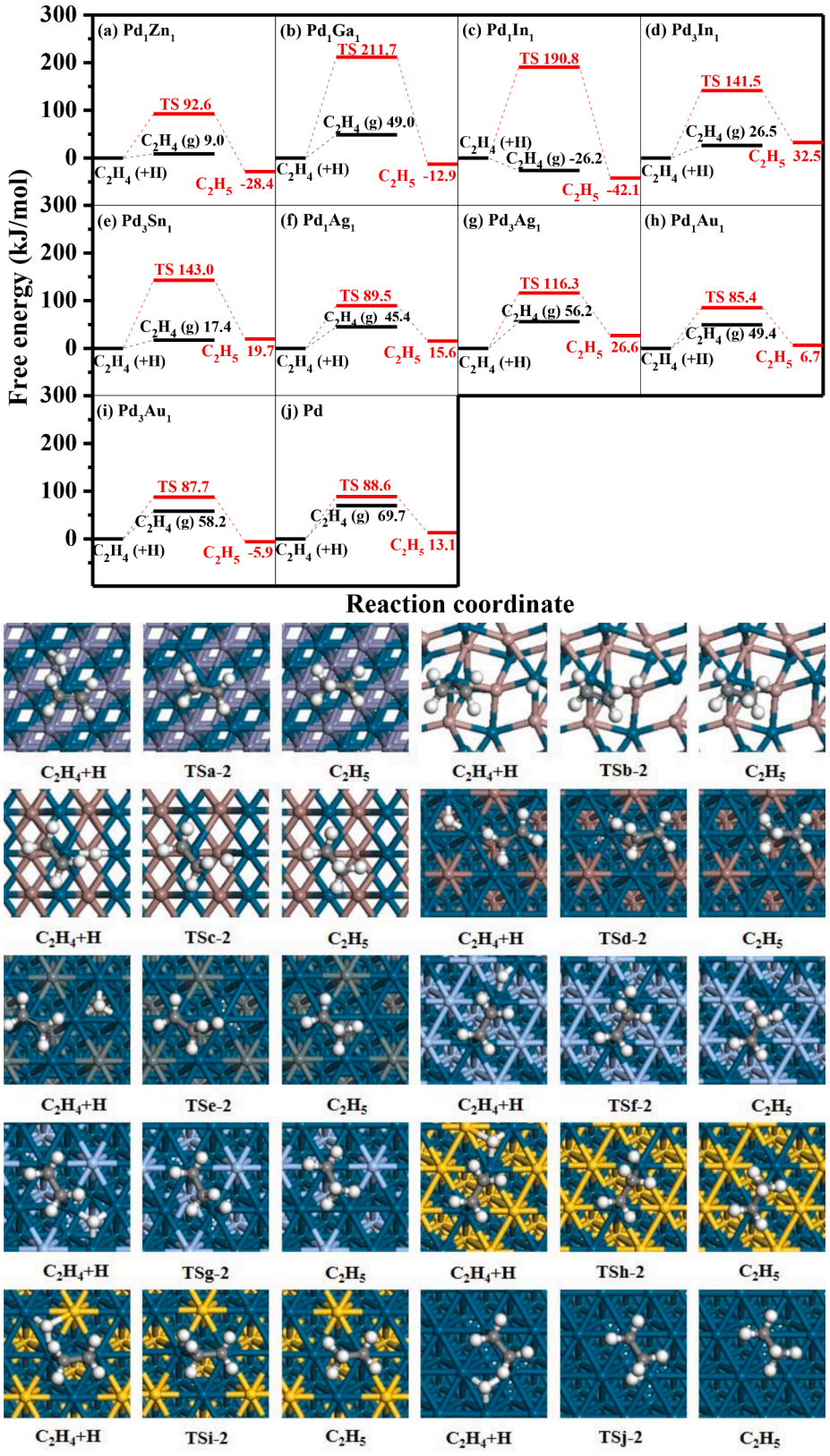

Fig. 5. The potential energy profile at 425 K of C_2H_4 hydrogenation and C_2H_4 desorption with the initial state, transition state and final state on the (a) Pd_1Zn_1, (b) Pd_1Ga_1, (c) Pd_1In_1, (d) Pd_3In_1, (e) Pd_3Sn_1, (f) Pd_1Ag_1, (g) Pd_3Ag_1, (h) Pd_1Au_1, (i) Pd_3Au_1 and (j) Pd, respectively.

Correspondingly, C_2H_4 formation activity is 2.57×10^0, 1.20×10^{-3}, 2.05×10^0, 1.23×10^{-5}, 9.38×10^{-2}, 2.30×10^{-3}, 3.17×10^{-1}, $\mathbf{4.77 \times 10^6}$, 4.41×10^0, 5.92×10^{-4}, 3.01×10^4, 5.12×10^2 and 3.55×10^{-1} $s^{-1}\cdot site^{-1}$, respectively. Thus, among the Pd_xN_y IMCs, Pd_1Cu_3 IMCs with the surface single-atom Pd as active center presents outstanding selectivity and activity (**122.3** $kJ\cdot mol^{-1}$ and $\mathbf{4.77 \times 10^6}\cdot s^{-1}\cdot site^{-1}$) for gaseous C_2H_4 formation.

3.3.5. The influences of partner metal ratio and metal type on C_2H_4 formation

Similarly, the influences of partner metal ratio and type in the Pd_xN_y(N = Zn, Ga, In, Sn, Cu, Ag and Au) IMCs on C_2H_4 formation activity and selectivity are also obvious. Among them, the Pd_xIn_y, Pd_xAg_y and Pd_xAu_y IMCs corresponding to Pd/In, Pd/Ag and Pd/Au ratio of 1/1 have superior C_2H_4 formation activity and selectivity than other Pd/N(N = In, Ag and Au) ratios. Similarly, the Pd_xZn_y and Pd_xGa_y IMCs also correspond to the Pd/Zn or Pd/Ga ratio of 1/1. However, Pd_xSn_y IMCs correspond to the Pd/Sn ratio of 3/1, and it is Pd/Cu ratio of 1/3 for Pd_xCu_y IMCs. Thus, the Pd_1Zn_1, Pd_1Ga_1, Pd_1In_1, Pd_1Ag_1, Pd_1Au_1, Pd_3Sn_1 and Pd_1Cu_3 IMCs favor the formation of gaseous C_2H_4.

Moreover, as shown in Fig. 6, the partner metal type N(N = Zn, Ga, In, Sn, Cu, Ag and Au) in Pd_xN_y IMCs affects C_2H_4 formation activity and selectivity, among them, Pd_1Cu_3 IMCs displays the highest activity and superior selectivity for C_2H_4 formation compared to other six types of Pd_xN_y IMCs catalysts, namely, Pd_1Cu_3 IMCs becomes the best choice for C_2H_2 selective hydrogenation among Pd_xN_y IMCs.

3.4. General discussions

3.4.1. The influences of partner metal ratio and type on C_2H_4 formation activity and selectivity

Noble-metal Pd has been industrially used to remove trace C_2H_2 from a large amount of C_2H_4 due to its high hydrogenation activity [8,64], aiming at obtaining the influences of partner metal ratio and type in the Cu_xM_y or Pd_xN_y IMCs on C_2H_4 formation activity and selectivity, the comparisons of the activity and selectivity between Cu_xM_y/Pd_xN_y IMCs and Pd catalysts are carried out.

For the Cu_xM_y IMCs, all considered catalysts exhibit better C_2H_4 selectivity ($kJ\cdot mol^{-1}$) compared to Pd catalyst, following the order of Cu_3Ag_1(133.1)> Cu_1Zn_1(130.3)>Cu_3Pd_1(122.3)>Cu_3Au_1(104.4)>Cu_3Zn_1(93.2)>Cu_3Pt_1(50.1)>Cu_1Pd_1(49.6)>Cu_1Pd_3(45.1)> Cu_3Ni_1(34.0)>Cu_1Ni_1(30.0)>Cu_1Pt_1(24.0)>Pd(18.9). The activity ($s^{-1}\cdot site^{-1}$) of C_2H_4 formation on the Cu_3Pd_1, Cu_1Pt_1, Cu_3Ni_1, Cu_3Ag_1 and Cu_3Zn_1 (4.77×10^6, 8.85×10^1, 1.33×10^1, 5.68×10^0 and 5.27×10^{-1}) is superior to that on Pd catalyst (3.55×10^{-1}). Thus, C_2H_4 formation activity and selectivity on five types of Cu_3Zn_1, Cu_1Pt_1, Cu_3Ni_1, Cu_3Pd_1 and Cu_3Ag_1 IMCs have a greater improvement compared to that on Pd catalyst. Among them, Cu_3Pd_1 that has the surface single-atom Pd as active center displays outstanding C_2H_4 formation activity and selectivity.

For the Pd_xN_y IMCs, C_2H_4 selectivity ($kJ\cdot mol^{-1}$) follows the order of Pd_1In_1(217.0)>Pd_1Ga_1(162.7)>Pd_3Sn_1(125.6)>Pd_1Cu_3(122.3)>Pd_3In_1(115.0)>Pd_1Zn_1 (83.6)>Pd_3Ag_1(60.1)>Pd_1Cu_1(49.6)> Pd_3Cu_1(45.1)>Pd_1Ag_1(44.1)>Pd_1Au_1(36.0)>Pd_3Au_1(29.5)>Pd (18.9). The activity ($s^{-1}\cdot site^{-1}$) of C_2H_4 formation on the Pd_1Cu_3, Pd_1Au_1, Pd_3Au_1, Pd_1Ag_1, Pd_1Zn_1 and Pd_1In_1 (4.77×10^6, 3.01×10^4, 5.12×10^2, 4.41×10^0, 2.57×10^0 and 2.05×10^0) is superior to that on Pd catalyst (3.55×10^{-1}). Namely, C_2H_4 formation activity and selectivity on six types of Pd_1Cu_3, Pd_1Au_1, Pd_3Au_1, Pd_1Ag_1, Pd_1Zn_1 and Pd_1In_1 IMCs have been greatly improved in comparison with that on Pd catalyst, among them, Pd_1Cu_3 IMCs corresponding to the isolated surface single-atom Pd active center exhibits excellent C_2H_4 formation activity and selectivity.

In general, as presented in Fig. 6, among all considered Cu_xM_y or Pd_xN_y IMCs in this study, Pd_xCu_y IMCs that has the Pd/Cu ratio of 1: 3 becomes the best choice for C_2H_2 hydrogenation to produce gaseous C_2H_4 with excellent activity and selectivity ($\mathbf{4.77 \times 10^6}$ $s^{-1}\cdot site^{-1}$ and **122.3** $kJ\cdot mol^{-1}$) in comparison with other Cu_xM_y or Pd_xN_y IMCs and Pd catalysts. Further, previous studies found that Cu exhibited low activity for alkyne hydrogenation [65,66]. The selectivity (13.0 $kJ\cdot mol^{-1}$) and activity (1.00×10^{-2} $s^{-1}\cdot site^{-1}$) of C_2H_4 formation on Cu catalyst at 425 K are much lower than those on Pd_1Cu_3 IMCs [67]. Moreover, PdCu(111) alloy surface doped by the single-atom Pd displays C_2H_4 selectivity of 39.8 $kJ\cdot mol^{-1}$, which is still much lower than

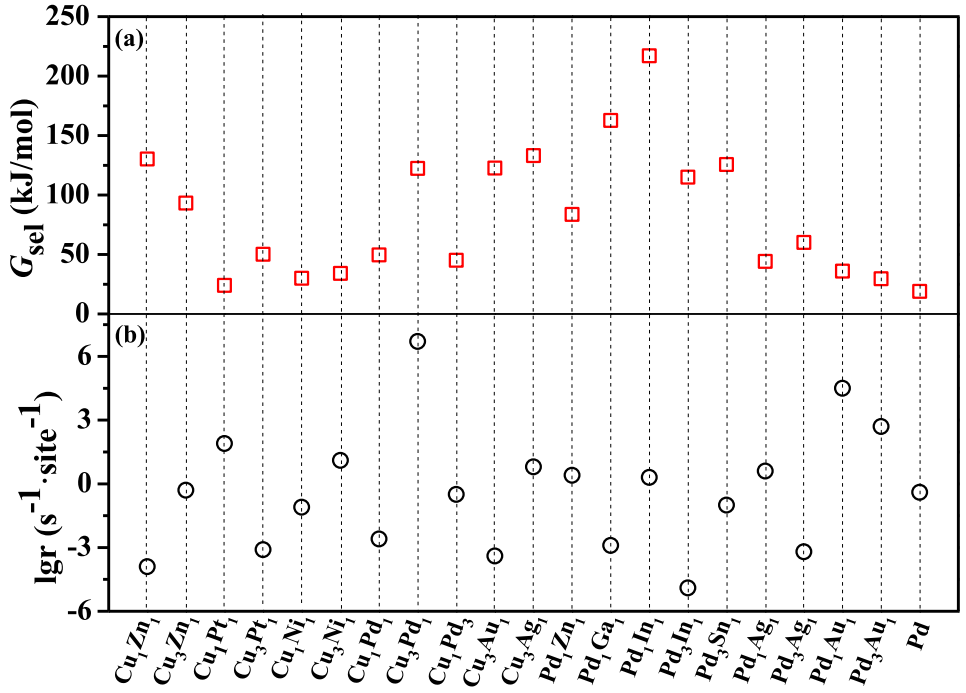

Fig. 6. (a) C_2H_4 selectivity and (b) C_2H_4 formation activity in C_2H_2 selective hydrogenation over the Cu_xM_y(M = Zn, Pt, Ni, Pd, Au, Ag) and Pd_xN_y(N = Zn, Ga, In, Sn, Cu, Ag, Au) IMCs and Pd catalysts at 425 K.

that on Pd_1Cu_3 IMCs [30]; meanwhile, PdCu(211) alloy surface doped by the single-atom Pd shows C_2H_4 formation activity of 1.58×10^4 $s^{-1}\cdot site^{-1}$ and its selectivity of 36.4 $kJ\cdot mol^{-1}$ in C_2H_2 selective hydrogenation [60], however, both are still much lower than those on Pd_1Cu_3 IMCs catalyst in this study.

Further, Wang *et al.* [68] studied C_2H_2 selective hydrogenation over the anatase and rutile supported Pd_4 cluster and found that the anatase one has higher C_2H_4 selectivity than the rutile one due to the easier C_2H_4 desorption and higher activation barriers of C_2H_4 hydrogenation. Guan *et al.* [69] investigated C_2H_2 selective hydrogenation over the supported Pd and Cu cluster with different supports, suggesting that the oxygen-vacancy anatase supported Pd_{19} cluster is the most favorable for gaseous C_2H_4 formation, but the activity (6.19×10^5 $s^{-1}\cdot site^{-1}$) is still much lower than that of Pd_1Cu_3 IMCs in our study. Meng *et al.* [57] reported C_2H_2 selective hydrogenation over the oxygen defective anatase supported Pd_4 and Pd_aAg_b(a + b = 4) clusters, indicating that the supported Pd_3Ag cluster displays the highest C_2H_4 selectivity (103.2 $kJ\cdot mol^{-1}$), which is still lower than that of Pd_1Cu_3 IMCs in our study. Therefore, Pd_1Cu_3 IMCs in this study is more favorable for C_2H_4 formation to remove traces C_2H_2 in comparison with the single Pd, Cu, the single-atom Pd-doped Cu alloy and the supported catalysts, which is attributed to well-defined surface atomic arrangement.

3.4.2. The influences of partner metal ratio and type on green oil production

Since the production of green oil can block active centers and deactivate the catalyst in C_2H_2 selective hydrogenation, we further analyze the production of green oil over the Cu_xM_y or Pd_xN_y IMCs screened out based on better activity and selectivity toward C_2H_4 formation in comparison with Pd catalyst.

For the Cu_xM_y IMCs, the production of green oil on five types of Cu_3Zn_1, Cu_1Pt_1, Cu_3Ni_1, Cu_3Pd_1 and Cu_3Ag_1 catalysts is investigated (see Fig. S15). On Cu_3Zn_1, see Fig. S15a, compared to the routes of C_2H_2+C_2H_2 (212.9 $kJ\cdot mol^{-1}$) and C_2H_2+C_2H_3 (238.9 $kJ\cdot mol^{-1}$), the route of C_2H_3+C_2H_3 to produce 1,3-butadiene is the most advantageous in kinetics (141.7 $kJ\cdot mol^{-1}$). The same thing also occurs on the Cu_3Pd_1, Cu_3Ag_1, Cu_1Pt_1 and Cu_3Ni_1 (see Figs. S15b~S15e). Further, as presented in Fig. 7, the route of C_2H_3+C_2H_3 to 1,3-butadiene is much easier in kinetics than C_2H_4 desorption route on the Cu_1Pt_1 (74.2 *vs.* 76.7 $kJ\cdot mol^{-1}$) and Cu_3Ni_1 (23.9 *vs.* 32.8 $kJ\cdot mol^{-1}$), respectively. However, C_2H_4 desorption route is much easier in kinetics than the route of C_2H_3+C_2H_3 to 1,3-butadiene on the Cu_3Zn_1 (98.5 *vs.* 174.6 $kJ\cdot mol^{-1}$), Cu_3Pd_1 (46.2 *vs.* 61.9 $kJ\cdot mol^{-1}$) and Cu_3Ag_1 (102.7 *vs.* 162.2 $kJ\cdot mol^{-1}$). Thus, green oil is easily produced on the Cu_1Pt_1 and Cu_3Ni_1, whereas Cu_3Zn_1, Cu_3Pd_1 and Cu_3Ag_1 can validly suppress green oil production.

For the Pd_xN_y IMCs, six types of Pd_1Cu_3, Pd_1Au_1, Pd_3Au_1, Pd_1Ag_1, Pd_1Zn_1 and Pd_1In_1 IMCs catalysts can greatly improve C_2H_4 formation activity and selectivity in comparison with that on Pd catalyst, since C_2H_4 formation activity and selectivity on Pd_1Au_1 is better than Pd_3Au_1, only Pd_1Au_1 is considered. The results on five types of Pd_1Zn_1, Pd_1In_1, Pd_1Ag_1, Pd_1Cu_3 and Pd_1Au_1 catalysts (see Fig. S16) indicate that the route of C_2H_3+C_2H_3 to produce 1,3-butadiene is the most advantageous on the Pd_1Zn_1, Pd_1Cu_3, Pd_1Ag_1 and Pd_1Au_1, while the route of C_2H_2+C_2H_3 is the most favorable on Pd_1In_1. Further, as shown in Fig. 7, the route of C_2H_3+C_2H_3 to 1,3-butadiene is difficult in kinetics compared to C_2H_4 desorption route on the Pd_1Zn_1 (176.4 *vs.* 56.3 $kJ\cdot mol^{-1}$), Pd_1In_1 (148.6 *vs.* 59.5 $kJ\cdot mol^{-1}$) and Pd_1Cu_3 (61.9 *vs.* 46.2 $kJ\cdot mol^{-1}$); however, it is opposite on the Pd_1Ag_1 (45.0 *vs.* 67.6 $kJ\cdot mol^{-1}$) and Pd_1Au_1 (39.0 *vs.* 59.8 $kJ\cdot mol^{-1}$). Hence, green oil production can be inhibited on the Pd_1Zn_1, Pd_1In_1 and Pd_1Cu_3 IMCs catalysts.

Based on above results for Cu_xM_y or Pd_xN_y IMCs, it is obtained that compared to Pd catalyst, five types of Cu_3Zn_1, Cu_3Pd_1, Cu_3Ag_1, Pd_1Zn_1 and Pd_1In_1 IMCs catalysts not only possess better C_2H_4 formation selectivity and activity, but also hinder green oil formation among the considered Cu_xM_y or Pd_xN_y IMCs catalysts.

3.4.3. The influences of partner metal ratio and type on H_2 dissociation

Since H_2 dissociation is the key step of C_2H_2 selective hydrogenation, the adsorption and dissociation of H_2 on above five types of Cu_xM_y and Pd_xN_y IMCs including Cu_3Zn_1, Cu_3Pd_1, Cu_3Ag_1, Pd_1Zn_1 and Pd_1In_1 IMCs were further investigated (see Figs. S17 and S18), which have better C_2H_4 formation activity and selectivity and the suppression ability toward the production of green oil compared to Pd catalyst. The results show that H_2 dissociative adsorption proceeds spontaneously on Cu_3Pd_1

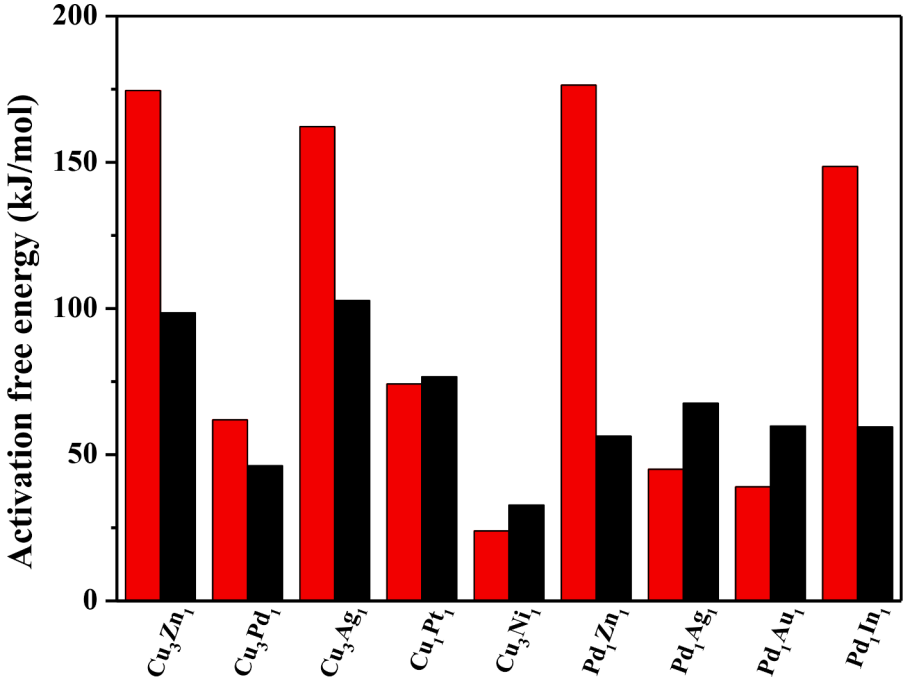

Fig. 7. The overall barriers of the optimal route for 1,3-butadiene formation (red column) and C_2H_4 formation (black column) in C_2H_2 selective hydrogenation over the Cu_3Zn_1, Cu_3Pd_1, Cu_3Ag_1, Cu_1Pt_1, Cu_3Ni_1, Pd_1Zn_1, Pd_1Ag_1, Pd_1Au_1 and Pd_1In_1 IMCs. (For interpretation of the references to color in this figure legend, the reader is referred to the web version of this article.)

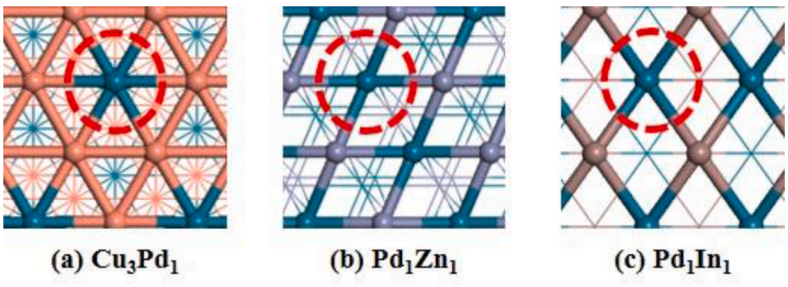

Fig. 8. The surface structures of (a) Cu_3Pd_1, (b) Pd_1Zn_1 and (c) Pd_1In_1 IMCs.

IMCs catalyst (see Fig. S17). However, H_2 molecular adsorption occurs on the Cu_3Zn_1, Cu_3Ag_1, Pd_1In_1 and Pd_1Zn_1 IMCs, correspondingly, H_2 dissociation barriers are 95.6, 113.5, 60.2 and 24.3 kJ·mol^{-1}, see Fig. S18, namely, the dissociation of H_2 into H atom also easily occurs on the latter two IMCs. Therefore, three types of Cu_3Pd_1, Pd_1Zn_1 and Pd_1In_1 IMCs catalysts can provide abundant hydrogen source to participate into C_2H_2 hydrogenation, especially, Cu_3Pd_1. In addition, H_2 dissociation is easy on the three-layer $p(3 \times 3)$ (111) surface of Cu_3Pd_1 IMCs [49]. Zhou *et al.* [20] experimentally and theoretically showed that PdZn IMCs promote H_2 dissociation.

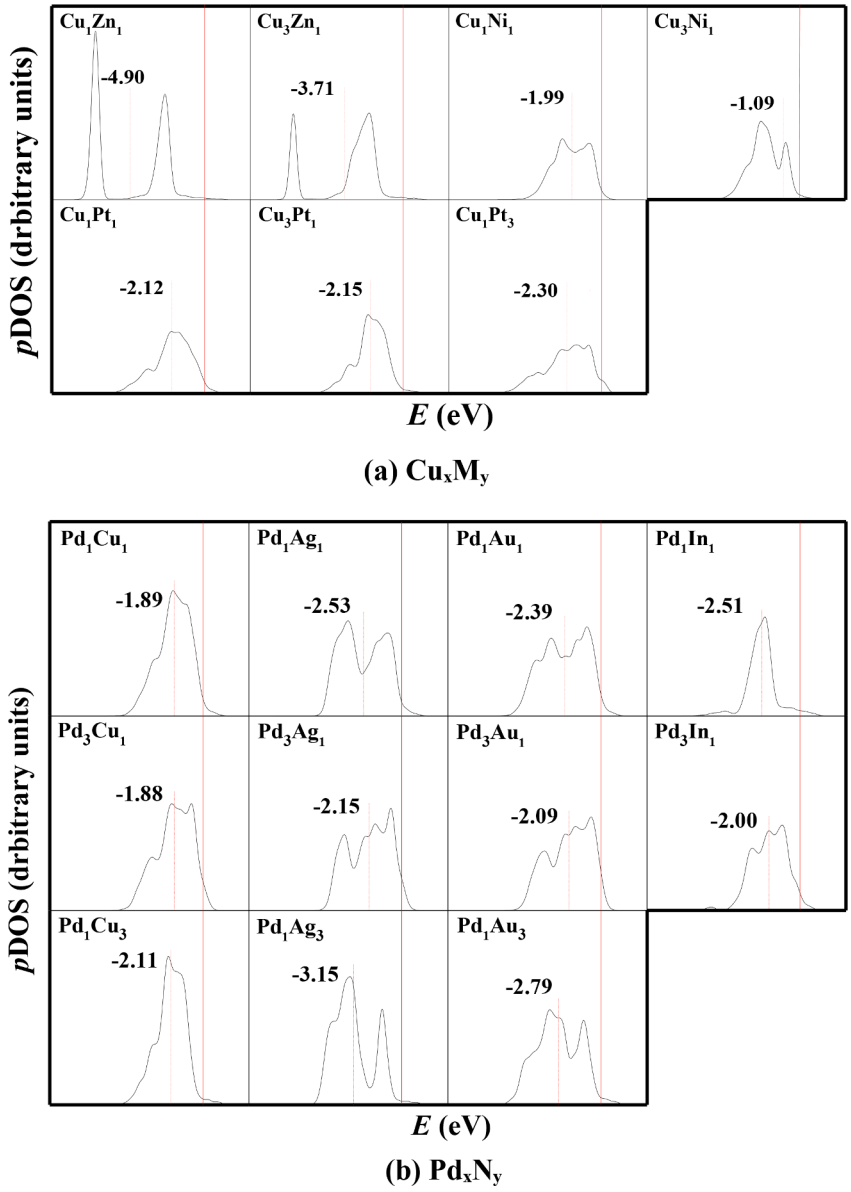

Fig. 9. Projected density of states (PDOS) plots for the *d*-orbitals of the outmost layer atoms over the (a) Cu_xM_y(M = Zn, Pt and Ni) IMCs and (b) Pd_xN_y(N = Cu, Ag, Au and In) IMCs. The dashed red lines represent the location of *d*-band center, and the solid red lines indicate Fermi energy level to be zero. (For interpretation of the references to color in this figure legend, the reader is referred to the web version of this article.)

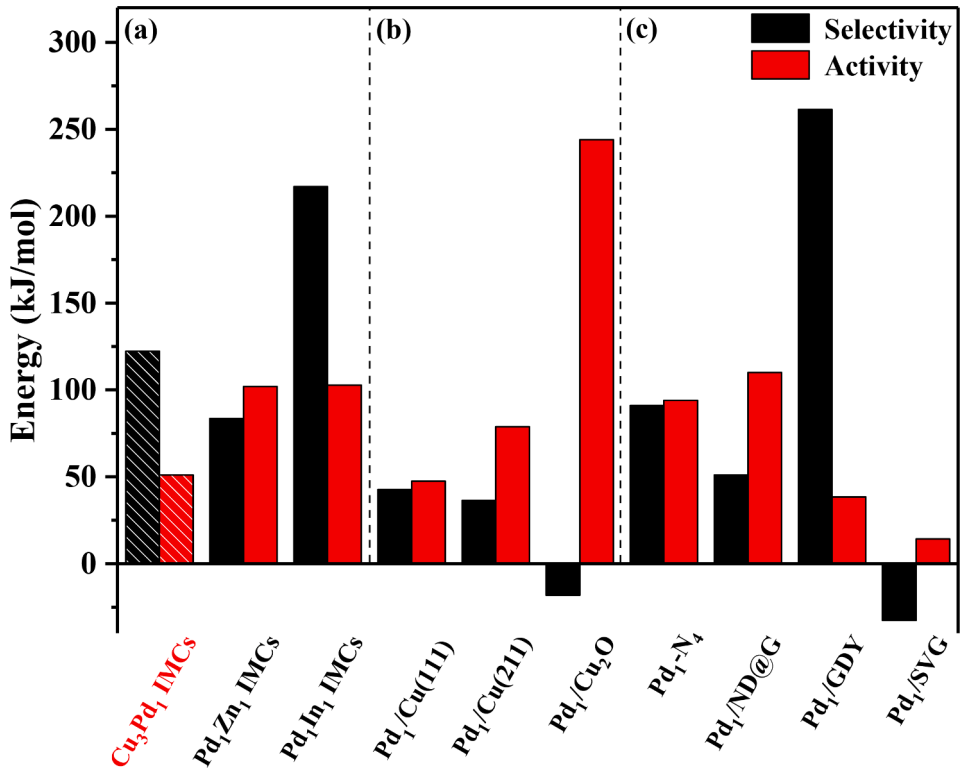

Fig. 10. Comparisons of C_2H_4 formation activity and selectivity between Cu_3Pd_1 IMCs and other previously reported single-atom Pd catalysts: (a) Intermetallic compounds, (b) alloy surfaces, (c) the supported catalysts. The black bar stands for C_2H_4 selectivity, and the red bar stands for the overall barrier of C_2H_4 formation to reflect the activity, respectively. (For interpretation of the references to color in this figure legend, the reader is referred to the web version of this article.)

3.4.4. The influences of partner metal ratio and type on surface structure

Taking C_2H_4 formation activity and selectivity, the suppression of green oil and H_2 dissociation activity on the Cu_xM_y or Pd_xN_y IMCs into consideration, the surface structures for three types of Cu_3Pd_1, Pd_1Zn_1 and Pd_1In_1 IMCs with better performance are analyzed. As shown in Fig. 8, it is obtained that only three types of Pd_1Zn_1, Pd_1In_1 and Cu_3Pd_1 IMCs with the surface isolated single-atom Pd active centers can facilitate the reaction of $C_2H_2+2H\rightarrow C_2H_4$. Meanwhile, the Pd_1Ag_3, Pd_1Au_3 and Pd_1Ga_1 IMCs also have the surface isolated single-atom Pd active centers, however, the close adsorption energies between C_2H_2 and C_2H_4 on the Pd_1Ag_3 and Pd_1Au_3 leads to poor catalytic performance, the low C_2H_4 formation activity limits C_2H_4 production on Pd_1Ga_1. Thus, different partner metal ratios and types alter surface structure of catalysts, and affect catalytic performance toward the reaction of $C_2H_2+2H\rightarrow C_2H_4$. In addition, theoretical studies showed that $PdCu_3$ IMCs with three-layer model enables high C_2H_4 formation activity and selectivity, and limits green oil production at 400 K [49]. Zhou *et al.* [20] experimentally and theoretically showed that PdZn IMCs is highly selective and active for C_2H_4 formation, however, the green oil production is not considered. Feng *et al.* [6] experimentally and theoretically indicated that Pd_1In_1 IMCs with the single-atom Pd active centers displays superior C_2H_4 selectivity without considering green oil production.

Therefore, among all considered Cu_xM_y or Pd_xN_y IMCs catalysts in this study, Cu_3Pd_1 IMCs with the surface isolated single-atom Pd active centers, namely, Pd_1Cu_3 IMCs catalyst, is the best choice for C_2H_2 selective hydrogenation, which not only exhibits high C_2H_4 formation activity and selectivity, but also inhibits green oil production and provides abundant hydrogen source for C_2H_2 selective hydrogenation. More importantly, Pd_1Cu_3 IMCs reduces the use of precious metal Pd compared to the widely used Pd-based catalysts. In addition, the defective nanodiamond-graphene catalyst supported the single-atom Pd presents high C_2H_4 selectivity [17]. Wei *et al.* [16] showed that the single-atom Pd fixed on the defects of nitrogen-doped carbon enables better C_2H_4 formation activity and selectivity.

3.4.5. The analysis of electronic properties

Aiming at further clarifying the roles of partner metal ratio and type in the Cu_xM_y and Pd_xN_y IMCs, the projected density of states for the *d*-orbitals of the outermost atoms of Cu_xM_y and Pd_xN_y IMCs facilitating C_2H_4 formation are analyzed.

For the Cu_xM_y IMCs, Cu_xM_y(M = Zn, Pt and Ni) is considered, as presented in Fig. 9a, the distance between the *d*-band center and Femi level follows the order: Cu_3Zn_1 (-3.71 eV)<Cu_1Zn_1 (-4.90 eV), Cu_1Pt_1 (-2.12 eV)<Cu_3Pt_1 (-2.15 eV)< Cu_1Pt_3 (-2.30 eV) and Cu_3Ni_1 (-1.09 eV)<Cu_1Ni_1 (-1.99 eV), suggesting that Cu_3Zn_1 catalyst with *d*-band center closer to Fermi level has superior activity than Cu_1Zn_1, the same things also occur on the Cu_xPt_y and Cu_xNi_y IMCs.

For the Pd_xN_y IMCs, as presented in Fig. 9b, Pd_xN_y(N = Ag, In, Cu and Au) is considered, the *d*-band center deviates the farthest from the Fermi level on the Pd_1Ag_3 and Pd_1Au_3 (-3.15 and -2.79 eV) catalysts without C_2H_4 production. For Pd_xIn_y, Pd_1In_1 catalyst with *d*-band center far away from the Fermi level has superior catalytic activity than Pd_3In_1 (-2.51 and -2.00 eV). The same things also occur on the Pd_xCu_y with the order of Pd_1Cu_3 (-2.11 eV)>Pd_1Cu_1 (-1.89 eV)>Pd_3Cu_1 (-1.88 eV), Pd_xAg_y with the order of Pd_1Ag_1 (-2.53 eV)>Pd_3Ag_1 (-2.15 eV) and Pd_xAu_y with the order of Pd_1Au_1 (-2.39 eV)>Pd_3Au_1 (-2.09 eV), suggesting that Pd_xN_y(N = Ag, In, Cu and Au) with the *d*-band center far away from the Fermi level have better catalytic activity for C_2H_2 selective hydrogenation. Zhao *et al.* [61] showed that Cu catalyst displays better C_2H_4 formation activity with the *d*-band center far away from the Fermi level.

Above results show that the different partner metal ratios of Cu_xM_y(M = Zn, Pt and Ni) and Pd_xN_y(N = Ag, In, Cu and Au) IMCs can alter the location of *d*-band center, and further influence C_2H_4 formation activity.

On the other hand, as presented in Section 3.4.4, taking C_2H_4 formation activity and selectivity, the suppression of green oil and H_2 dissociation activity over the Cu_xM_y or Pd_xN_y into consideration, among them, three types of Cu_3Pd_1, Pd_1Zn_1 and Pd_1In_1 IMCs are the best choice for

C_2H_2 selective hydrogenation to C_2H_4, especially, Cu_3Pd_1; Further, Cu_3Pd_1 IMCs with the *d*-band center closer to the Fermi level possesses the highest C_2H_4 formation activity. Thus, different partner metal types of Cu_xM_y or Pd_xN_y IMCs can also change the location of *d*-band center, and further influence C_2H_4 formation activity.

3.4.6. Catalytic performance comparisons between Cu_3Pd_1 IMCs and the previously reported catalysts

In order to further explain outstanding selectivity and activity of Cu_3Pd_1 IMCs with surface Pd single-atom, the comparisons about C_2H_4 formation activity and selectivity between Cu_3Pd_1 IMCs and previously reported catalysts were performed.

As presented in Fig. 10a, our results showed that on Cu_3Pd_1, C_2H_4 selectivity is 122.3 kJ·mol^{-1}, and the activation barriers of C_2H_2+H→C_2H_3 and C_2H_3+H→C_2H_4 are 51.0 and 46.2 kJ·mol^{-1}, respectively; the overall barrier of C_2H_2 hydrogenation to C_2H_4 is 51.0 kJ·mol^{-1}. Pd_1Zn_1 has C_2H_4 selectivity (83.6 kJ·mol^{-1}), and the activation barriers of C_2H_2+H→C_2H_3 and C_2H_3+H→C_2H_4 are 102.0 and 56.3 kJ·mol^{-1}, respectively. Pd_1In_1 corresponding to the surface single-atom Pd as the active centers displays high C_2H_4 selectivity (217.0 kJ·mol^{-1}), and the activation barriers of C_2H_2+H→C_2H_3 and C_2H_3+H→C_2H_4 are 102.8 and 59.5 kJ·mol^{-1}, respectively. Thus, in this study, compared to Pd_1Zn_1 and Pd_1In_1, the Cu_3Pd_1 has higher C_2H_4 formation activity and potential C_2H_4 selectivity.

As presented in Fig. 10b, for the surface alloys doped by Pd single-atom, Zhang *et al.* [59,60] found that C_2H_4 selectivity is 42.6 and 36.4 kJ·mol^{-1} on the PdCu(111) and PdCu(211) doped by Pd single-atom, respectively; the overall barriers of C_2H_2 hydrogenation to C_2H_4 are 47.5 and 78.8 kJ·mol^{-1}, respectively. However, ethane formation is easy on Pd-doped Cu_2O(111). In addition, ethane is easily formed on the single-atom Pd-doped Cu_{13}, Cu_{38} or Cu_{55} clusters in C_2H_2 selective hydrogenation [70]. C_2H_4 is easily over-hydrogenated to generate ethane on the PdAg(111) doped by Pd single-atom [71] and Pd_1M@Pd(111)(M = Cu, Au and Ag) [8]. Hence, the alloy surfaces doped by Pd single-atom as reported above still present lower C_2H_4 formation activity and selectivity compared to Cu_3Pd_1 in this study.

As presented in Fig. 10c, C_2H_4 selectivity over the stable catalyst with Pd single-atom fixed on the defects of nitrogen-doped carbon is 91.0 kJ·mol^{-1}, and the overall barrier of C_2H_2+2H→C_2H_4 is 94.0 kJ·mol^{-1} [16]. The catalyst with Pd single-atom dispersed onto the defective nanodiamond-graphene has C_2H_4 selectivity of 51.0 kJ·mol^{-1}, and the overall barriers of C_2H_2+2H→C_2H_4 is 110.0 kJ·mol^{-1} [17]. The catalyst with the atom-dispersed Pd onto nitrogen-doped graphene has C_2H_4 selectivity of 88.0 kJ·mol^{-1} [72]. Pd_1/SVG catalyst with Pd single-atom supported by a single vacancy graphene facilitates ethane formation [73]. Interestingly, Pd_1/GDY catalyst with Pd single-atom supported on the graphdiyne presents significantly high C_2H_4 selectivity (261.4 kJ·mol^{-1}) with the overall barriers of 38.4 kJ·mol^{-1} for C_2H_4 formation [73]. As a result, except for Pd_1/GDY catalyst, the other supported single-atom Pd catalysts mentioned above still exhibit lower activity and selectivity toward C_2H_4 formation compared to Cu_3Pd_1 IMCs in this study. Moreover, although Pd_1/GDY catalyst presents better C_2H_4 selectivity and formation activity than Cu_3Pd_1 IMCs, Cu_3Pd_1 IMCs with ordered atomic arrangement and structural characteristics presents stronger thermal stability than the single-atom Pd_1/GDY catalyst.

Thus, the Cu_3Pd_1 or Pd_1Cu_3 may become a promising catalyst in C_2H_2 selective hydrogenation, which not only presents the industrially practical C_2H_4 formation activity and selectivity, but also possesses outstanding thermal stability.

4. Conclusions

In this work, aiming at reveal the most suitable partner metal type and ratio among the Cu_xM_y and Pd_xN_y IMCs and further screen out the most suitable IMCs with excellent catalytic performance for C_2H_2 selective hydrogenation, density functional theory calculations were performed to systematically investigate the underlying mechanism of C_2H_2 selective hydrogenation on the different types of Cu_xM_y(M = Zn, Pt, Ni, Pd, Au and Ag) or Pd_xN_y(N = Zn, Ga, In, Sn, Cu, Ag and Au) IMCs catalyst. This study examined the influences of the partner metal ratio and type in the Cu_xM_y and Pd_xN_y IMCs on the four key factors of C_2H_2 selective hydrogenation, including C_2H_4 formation activity and selectivity, green oil production and H_2 dissociation activity. Taking above four factors into account, the results reveal that either Cu_3Pd_1 or Pd_1Cu_3 IMCs with the surface isolated single-atom Pd anchored into IMCs bulk performed as active centers should be the most suitable intermetallic compound among the Cu_xM_y and Pd_xN_y IMCs, which presents the industrially practical performance for C_2H_4 formation in comparison with the previously reported single-atom Pd catalysts in experimental and theoretical studies. The excellent performance of Cu_3Pd_1 IMCs catalyst for C_2H_4 formation is attributed to the unique surface structures and electronic properties. Meanwhile, compared to the widely used Pd-based catalysts, the Cu_3Pd_1 or Pd_1Cu_3 IMCs with the surface isolated single-atom Pd catalyst not only reduces the cost of catalysts with the non-noble metal Cu as the main body, but also maximizes the utilization of noble metal Pd. This study provides valuable information for the design and screening out of intermetallic compound catalysts in selective hydrogenation of alkynes.

CRediT authorship contribution statement

Wenjuan Zheng: Writing – original draft, Writing – review & editing, Formal analysis. **Lixuan Ma:** Formal analysis, Data curation. **Baojun Wang:** Formal analysis, Data curation, Supervision, Software. **Jungang Wang:** Formal analysis, Conceptualization. **Riguang Zhang:** Writing – original draft, Writing – review & editing, Data curation, Conceptualization, Funding acquisition, Resources, Software, Project administration, Supervision.

Declaration of Competing Interest

The authors declare that they have no known competing financial interests or personal relationships that could have appeared to influence the work reported in this paper.

Acknowledgments

This work is financially supported by the National Natural Science Foundation of China (Nos. 21776193 and 22078221).

Supplementary materials

Supplementary material associated with this article can be found, in the online version, at doi:10.1016/j.mcat.2021.111660.

References

[1] Z.J. Zhao, J. Zhao, X. Chang, S. Zha, L. Zeng, J. Gong, Competition of C-C bond formation and C-H bond formation for acetylene hydrogenation on transition metals: A density functional theory study, AIChE J. 65 (2019) 1059–1066.
[2] E. Vignola, S.N. Steinmann, A. Al Farra, B.D. Vandegehuchte, D. Curulla, P. Sautet, Evaluating the risk of C-C bond formation during selective hydrogenation of acetylene on palladium, ACS Catal. 8 (2018) 1662–1671.
[3] C. Yang, G. Wang, A. Liang, Y. Yue, H. Peng, D. Cheng, Understanding the role of Au in the selective hydrogenation of acetylene on trimetallic PdAgAu catalytic surface, Catal. Commun. 124 (2019) 41–45.
[4] A.J. McCue, J.A. Anderson, Recent advances in selective acetylene hydrogenation using palladium containing catalysts, Front. Chem. Sci. Eng. 9 (2015) 142–153.
[5] J. Feng, Y. Liu, M. Yin, Y. He, J. Zhao, J. Sun, D. Li, Preparation and structure-property relationships of supported trimetallic PdAuAg catalysts for the selective hydrogenation of acetylene, J. Catal. 344 (2016) 854–864.
[6] Q. Feng, S. Zhao, Y. Wang, J. Dong, W. Chen, D. He, D. Wang, J. Yang, Y. Zhu, H. Zhu, L. Gu, Z. Li, Y. Liu, R. Yu, J. Li, Y. Li, Isolated single-atom Pd sites in intermetallic nanostructures: High catalytic selectivity for semihydrogenation of alkynes, J. Am. Chem. Soc. 139 (2017) 7294–7301.
[7] D. Teschner, J. Borsodi, A. Wootsch, Z. Révay, M. Hävecker, A. Knop-Gericke, S. D. Jackson, R. Schlögl, The roles of subsurface carbon and hydrogen in palladium-catalyzed alkyne hydrogenation, Science 320 (2008) 86–89.

[8] B. Yang, R. Burch, C. Hardacre, G. Headdock, P. Hu, Influence of surface structures, subsurface carbon and hydrogen, and surface alloying on the activity and selectivity of acetylene hydrogenation on Pd surfaces: a density functional theory study, J. Catal. 305 (2013) 264–276.

[9] B. Bridier, N. López, J. Pérez-Ramírez, Partial hydrogenation of propyne over copper-based catalysts and comparison with nickel-based analogues, J. Catal. 269 (2010) 80–92.

[10] A.J. McCue, C.J. McRitchie, A.M. Shepherd, J.A. Anderson, Cu/Al_2O_3 catalysts modified with Pd for selective acetylene hydrogenation, J. Catal. 319 (2014) 127–135.

[11] Y. Liu, Y. He, D. Zhou, J. Feng, D. Li, Catalytic performance of Pd-promoted Cu hydrotalcite-derived catalysts in partial hydrogenation of acetylene: effect of Pd-Cu alloy formation, Catal. Sci. Technol. 6 (2016) 3027–3037.

[12] G.X. Pei, X.Y. Liu, X. Yang, L. Zhang, A. Wang, L. Li, H. Wang, X. Wang, T. Zhang, Performance of Cu-alloyed Pd single-atom catalyst for semihydrogenation of acetylene under simulated front-end conditions, ACS Catal. 7 (2017) 1491–1500.

[13] F. Studt, F. Abild-Pedersen, T. Bligaard, R.Z. Sørensen, C.H. Christensen, J. K. Nørskov1, Identification of non-precious metal alloy catalysts for selective hydrogenation of acetylene, Science 320 (2008) 1320–1323.

[14] Y. Cao, Z. Sui, Y. Zhu, X. Zhou, D. Chen, Selective hydrogenation of acetylene over $Pd\text{-}In/Al_2O_3$ catalyst: Promotional effect of indium and composition-dependent performance, ACS Catal. 7 (2017) 7835–7846.

[15] X. Shi, Y. Lin, L. Huang, Z. Sun, Y. Yang, X. Zhou, E. Vovk, X. Liu, X. Huang, M. Sun, S. Wei, J. Lu, Copper catalysts in semihydrogenation of acetylene: From single atoms to nanoparticles, ACS Catal. 10 (2020) 3495–3504.

[16] S. Wei, A. Li, J.C. Liu, Z. Li, W. Chen, Y. Gong, Q. Zhang, W.C. Cheong, Y. Wang, L. Zheng, H. Xiao, C. Chen, D. Wang, Q. Peng, L. Gu, X. Han, J. Li, Y. Li, Direct observation of noble metal nanoparticles transforming to thermally stable single atoms, Nat. Nanotechnol. 13 (2018) 856–861.

[17] F. Huang, Y. Deng, Y. Chen, X. Cai, M. Peng, Z. Jia, P. Ren, D. Xiao, X. Wen, N. Wang, H. Liu, D. Ma, Atomically dispersed Pd on nanodiamond/graphene hybrid for selective hydrogenation of acetylene, J. Am. Chem. Soc. 140 (2018) 13142–13146.

[18] Y. Zhao, M. Zhu, L. Kang, The DFT study of single-atom $Pd_1/g\text{-}C_3N_4$ catalyst for selective acetylene hydrogenation reaction, Catal. Lett. 148 (2018) 2992–3002.

[19] J. Li, Q. Guan, H. Wu, W. Liu, Y. Lin, Z. Sun, X. Ye, X. Zheng, H. Pan, J. Zhu, S. Chen, W. Zhang, S. Wei, J. Lu, Highly active and stable metal single-atom catalysts achieved by strong electronic metal-support interactions, J. Am. Chem. Soc. 141 (2019) 14515–14519.

[20] H. Zhou, X. Yang, L. Li, X. Liu, Y. Huang, X. Pan, A. Wang, J. Li, T. Zhang, PdZn intermetallic nanostructure with Pd-Zn-Pd ensembles for highly active and chemoselective semi-hydrogenation of acetylene, ACS Catal. 6 (2016) 1054–1061.

[21] C. Li, Y. Chen, S. Zhang, S. Xu, J. Zhou, F. Wang, M. Wei, D.G. Evans, X. Duan, Ni-In intermetallic nanocrystals as efficient catalysts toward unsaturated aldehydes hydrogenation, Chem. Mater. 25 (2013) 3888–3896.

[22] Y. Liu, J. Zhao, J. Feng, Y. He, Y. Du, D. Li, Layered double hydroxide-derived Ni-Cu nanoalloy catalysts for semi-hydrogenation of alkynes: Improvement of selectivity and anti-coking ability via alloying of Ni and Cu, J. Catal. 359 (2018) 251–260.

[23] D.M. Rao, S.T. Zhang, C.M. Li, Y. Di Chen, M. Pu, H. Yan, M. Wei, The reaction mechanism and selectivity of acetylene hydrogenation over Ni-Ga intermetallic compound catalysts: A density functional theory study, Dalt. Trans. 47 (2018) 4198–4208.

[24] Z. Wang, G. Wang, C. Louis, L. Delannoy, Novel non-noble bimetallic $Cu\text{-}Zn/TiO_2$ catalysts for selective hydrogenation of butadiene, J. Catal. 347 (2017) 185–196.

[25] A. Han, J. Zhang, W. Sun, W. Chen, S. Zhang, Y. Han, Q. Feng, L. Zheng, L. Gu, C. Chen, Q. Peng, D. Wang, Y. Li, Isolating contiguous Pt atoms and forming Pt-Zn intermetallic nanoparticles to regulate selectivity in 4-nitrophenylacetylene hydrogenation, Nat. Commun. 10 (2019), 3787-1–7.

[26] Y. Liu, X. Liu, Q. Feng, D. He, L. Zhang, C. Lian, R. Shen, G. Zhao, Y. Ji, D. Wang, G. Zhou, Y. Li, Intermetallic Ni_xM_y(M=Ga and Sn) nanocrystals: A non-precious metal catalyst for semi-hydrogenation of alkynes, Adv. Mater. 28 (2016) 4747–4754.

[27] M. Sandoval, P. Bechthold, V. Orazi, E.A. González, A. Juan, P.V. Jasen, The role of Ga in the acetylene adsorption on PdGa intermetallic, Appl. Surf. Sci. 435 (2018) 568–573.

[28] X. Nie, X. Jiang, H. Wang, W. Luo, M.J. Janik, Y. Chen, X. Guo, C. Song, Mechanistic understanding of alloy effect and water promotion for Pd-Cu bimetallic catalysts in CO_2 hydrogenation to methanol, ACS Catal 8 (2018) 4873–4892.

[29] Z.J. Zuo, X.Y. Gao, P. De Han, S.Z. Liu, W. Huang, Density functional theory (DFT) and kinetic monte carlo (KMC) study of the reaction mechanism of hydrogen production from methanol on ZnCu(111), J. Phys. Chem. C 120 (2016) 27500–27508.

[30] R. Zhang, J. Zhang, Z. Jiang, B. Wang, M. Fan, The cost-effective Cu-based catalysts for the efficient removal of acetylene from ethylene: the effects of Cu valence state, surface structure and surface alloying on the selectivity and activity, Chem. Eng. J. 351 (2018) 732–746.

[31] B. Hammer, L.B. Hansen, J.K. Nørskov, Improved adsorption energetics within density-functional theory using revised Perdew-Burke-Ernzerhof functionals, Phys. Rev. B 59 (1999) 7413–7421.

[32] J.P. Perdew, K. Burke, M. Ernzerhof, Generalized gradient approximation made simple, Phys. Rev. Lett. 77 (1996) 3865–3868.

[33] Y. Inada, H. Orita, Efficiency of numerical basis sets for predicting the binding energies of hydrogen bonded complexes: evidence of small basis set superposition error compared to gaussian basis sets, J. Comput. Chem. 29 (2008) 225–232.

[34] C. Zhou, J. Wu, A. Nie, R.C. Forrey, A. Tachibana, H. Cheng, On the sequential hydrogen dissociative chemisorption on small platinum clusters: a density functional theory study, J. Phys. Chem. C 111 (2007) 12773–12778.

[35] B. Wang, L. Song, R. Zhang, The dehydrogenation of CH_4 on Rh(111), Rh(110) and Rh(100) surfaces: a density functional theory study, Appl. Surf. Sci. 258 (2012) 3714–3722.

[36] X.M. Chen, B. Yang, D.P. Tao, Y.N. Dai, Theory study of AlCl disproportionation reaction mechanism on Al(110) surface, Metall. Mater. Trans. B 41 (2010) 137–145.

[37] L. Xu, E.E. Stangland, M. Mavrikakis, Ethylene versus ethane: a DFT-based selectivity descriptor for efficient catalyst screening, J. Catal. 362 (2018) 18–24.

[38] Y. Huang, Z. Liu, DFT study on hydrogen and sulfur adsorption on (111) surface of Pd, Cu, Au, and PdAu, PdCu alloys, Acta. Phys. Chim. Sin. 24 (2008) 1662–1668.

[39] M. Okada, Y. Tsuda, K. Oka, K. Kojima, W.A. Diño, A. Yoshigoe. H. Kasai, Experimental and theoretical studies on oxidation of Cu-Au alloy surfaces: Effect of bulk Au concentration, Sci. Rep. 6 (2016), 31101-1–8.

[40] R. Zhang, X. Guo, B. Wang, L. Ling, Insight into the effect of CuNi(111) and FeNi (111) surface structure and second metal composition on surface carbon elimination by O or OH: A comparison study with Ni(111) surface, J. Phys. Chem. C 119 (2015) 14135–14144.

[41] P. Hirunsit, W. Soodsawang, J. Limtrakul, CO_2 electrochemical reduction to methane and methanol on copper-based alloys: theoretical insight, J. Phys. Chem. C 119 (2015) 8238–8249.

[42] T. Adit Maark, B.R.K. Nanda, CO and CO_2 electrochemical reduction to methane on Cu, Ni, and $Cu_3Ni(211)$ surfaces, J. Phys. Chem. C 120 (2016) 8781–8789.

[43] M.M.J. Li, J. Zheng, J. Qu, F. Liao, E. Raine, W.C.H. Kuo, S.S. Su, P. Po, Y. Yuan, S. C.E. Tsang, The remarkable activity and stability of a highly dispersive beta-brass Cu-Zn catalyst for the production of ethylene glycol, Sci. Rep. 6 (2016) 4–11.

[44] Q.L. Tang, X.X. Duan, B. Liu, A.Q. Wei, S.L. Liu, Q. Wang, Y.P. Liang, X.H. Ma, A density functional study on properties of a Cu_3Zn material and CO adsorption onto its surfaces, Appl. Surf. Sci. 363 (2016) 128–139.

[45] Z.X. Chen, K.M. Neyman, A.B. Gordienko, N. Rösch, Surface structure and stability of PdZn and PtZn alloys: Density-functional slab model studies, Phys. Rev. B 68 (2003), 075417-1–8.

[46] Z. Wu, E.C. Wegener, H.T. Tseng, J.R. Gallagher, J.W. Harris, R.E. Diaz, Y. Ren, F. H. Ribeiro, J.T. Miller, Pd-In intermetallic alloy nanoparticles: highly selective ethane dehydrogenation catalysts, Catal. Sci. Technol. 6 (2016) 6965–6976.

[47] J. Zhao, S. Zha, R. Mu, Z.J. Zhao, J. Gong, Coverage effect on the activity of the acetylene semihydrogenation over Pd-Sn catalysts: a density functional theory study, J. Phys. Chem. C 122 (2018) 6005–6013.

[48] B. Yang, R. Burch, C. Hardacre, P. Hu, P. Hughes, Mechanistic study of 1,3-butadiene formation in acetylene hydrogenation over the Pd-based catalysts using density functional calculations, J. Phys. Chem. C 118 (2014) 1560–1567.

[49] Y. Wang, W. Zheng, B. Wang, L. Ling, R. Zhang, The effects of doping metal type and ratio on the catalytic performance of C_2H_2 semi-hydrogenation over the intermetallic compound-containing Pd catalysts, Chem. Eng. Sci. 229 (2021), 116131-1–14.

[50] F. Studt, F. Abild-Pedersen, T. Bligaard, R.Z. Sørensen, C.H. Christensen, J. K. Nørskov, On the role of surface modifications of palladium catalysts in the selective hydrogenation of acetylene, Angew. Chem. 120 (2008) 9439–9442.

[51] B. Yang, R. Burch, C. Hardacre, P. Hu, P. Hughes, Selective hydrogenation of acetylene over Cu(211), Ag(211) and Au(211): Horiuti-Polanyi mechanism: vs. non-Horiuti-Polanyi mechanism, Catal. Sci. Technol. 7 (2017) 1508–1514.

[52] B. Yang, R. Burch, C. Hardacre, G. Headdock, P. Hu, Origin of the increase of activity and selectivity of nickel doped by Au, Ag, and Cu for acetylene hydrogenation, ACS Catal. 2 (2012) 1027–1032.

[53] B. Yang, R. Burch, C. Hardacre, P. Hu, P. Hughes, Selective hydrogenation of acetylene over Pd-Boron catalysts: A density functional theory study, J. Phys. Chem. C 118 (2014) 3664–3671.

[54] B. Yang, R. Burch, C. Hardacre, P. Hu, P. Hughes, Importance of surface carbide formation on the activity and selectivity of Pd surfaces in the selective hydrogenation of acetylene, Surf. Sci. 646 (2016) 45–49.

[55] A. Hook, F.E. Celik, Predicting selectivity for ethane dehydrogenation and coke formation pathways over model Pt-M surface alloys with ab initio and scaling method, J. Phys. Chem. C. 121 (2017) 17882–17892.

[56] M. Krajčí, J. Hafner, Selective semi-hydrogenation of acetylene: atomistic scenario for reactions on the polar threefold surfaces of GaPd, J. Catal. 312 (2014) 232–248.

[57] L.D. Meng, G.C. Wang, A DFT+U study of acetylene selective hydrogenation over anatase supported Pd_aAg_b (a+b=4) cluster, Phys. Chem. Chem. Phys. 16 (2014) 17541–17550.

[58] H.Y. Ma, G.C. Wang, Selective hydrogenation of acetylene on Pt_n/TiO_2(n=1, 2, 4, 8) surfaces: structure sensitivity analysis, ACS Catal. 10 (2020) 4922–4928.

[59] R. Zhang, J. Zhang, B. Zhao, L. He, A. Wang, B. Wang, Insight into the effects of Cu component and the promoter on the selectivity and activity for efficient removal of acetylene from ethylene on Cu-based catalyst, J. Phys. Chem. C 121 (2017) 27936–27949.

[60] R. Zhang, B. Zhao, L. He, A. Wang, B. Wang, Cost-effective promoter-doped Cu-based bimetallic catalysts for the selective hydrogenation of C_2H_2 to C_2H_4: The effect of the promoter on selectivity and activity, Phys. Chem. Chem. Phys. 20 (2018) 17487–17496.

[61] B. Zhao, R. Zhang, Z. Huang, B. Wang, Effect of the size of Cu clusters on selectivity and activity of acetylene selective hydrogenation, Appl. Catal. A: Gen. 546 (2017) 111–121.

[62] R. Zhang, M. Peng, L. Ling, B. Wang, PdIn intermetallic material with isolated single-atom Pd sites—a promising catalyst for direct formic acid fuel cell, Chem. Eng. Sci. 199 (2019) 64–78.

[63] Y. Yang, L. Chen, Y. Chen, W. Liu, H. Feng, B. Wang, X. Zhang, M. Wei, The selective hydrogenation of furfural over intermetallic compounds with outstanding catalytic performance, Green Chem. 21 (2019) 5352–5362.
[64] D. Mei, M. Neurock, C.M. Smith, Hydrogenation of acetylene-ethylene mixtures over Pd and Pd-Ag alloys: First-principles-based kinetic Monte Carlo simulations, J. Catal. 268 (2009) 181–195.
[65] N. J.Ossipoff, N.W. Cant, The hydrogenation and oligomerisation or ropyne ovean ion-exchanged copper on slica catalyst, J. Catal. 148 (1994) 125–133.
[66] R.A. Koeppel, J.T. Wehrli, M.S. Wainwright, D.L. Trimma, N.W. Cant, Selective hydrogenation of C_4-alkynes over a copper on silica catalyst, Appl. Catal. A 120 (1994) 163–177.
[67] R. Zhang, B. Zhao, L. Ling, A. Wang, C.K. Russell, B. Wang, M. Fan, Cost-effective palladium-doped Cu bimetallic materials to tune selectivity and activity by using doped atom ensembles as active sites for efficient removal of acetylene from ethylene, Chem. Cat. Chem. 10 (2018) 2424–2432.
[68] J. Yang, C.Q. Lv, Y. Guo, G.C. Wang, A DFT+U study of acetylene selective hydrogenation on oxygen defective anatase (101) and rutile (110) TiO_2 supported Pd_4 cluster, J. Chem. Phys. 136 (2012), 104107.
[69] Z. Guan, M. Xue, Z. Li, R. Zhang, B. Wang, C_2H_2 semi-hydrogenation over the supported Pd and Cu catalysts: the effects of the support types, properties and metal-support interaction on C_2H_4 selectivity and activity, Appl. Surf. Sci. 503 (2020), 144142.
[70] R. Zhang, M. Xue, B. Wang, L. Ling, Acetylene selective hydrogenation over different size of Pd-modified Cu cluster catalysts: effects of Pd ensemble and cluster size on the selectivity and activity, Appl. Surf. Sci. 481 (2019) 421–432.
[71] Y. Wang, B. Wang, L. Ling, R. Zhang, M. Fan, Probe into the effects of surface composition and ensemble effect of active sites on the catalytic performance of C_2H_2 semi-hydrogenation over the Pd-Ag bimetallic catalysts, Chem. Eng. Sci. 218 (2020), 115549-1–13.
[72] S. Zhou, L. Shang, Y. Zhao, R. Shi, G.I.N. Waterhouse, Y.C. Huang, L. Zheng, T. Zhang, Pd single-atom catalysts on nitrogen-doped graphene for the highly selective photothermal hydrogenation of acetylene to ethylene, Adv. Mater. 31 (2019), 1900509-1–7.
[73] Y. Wang, Y. Qi, M. Fan, B. Wang, L. Ling, R. Zhang, C_2H_2 semi-hydrogenation on the Pd_xM_y cluster/graphdiyne catalysts: effects of cluster composition and size on the activity and selectivity. Green Energy Environ (2021) https://doi.org/10.1016/j.gee.2020.10.020.